Available online at www.sciencedirect.com

ScienceDirect

Geochimica et Cosmochimica Acta xxx (2018) xxx–xxx

Geochimica et Cosmochimica Acta

www.elsevier.com/locate/gca

Quantifying early marine diagenesis in shallow-water carbonate sediments

Anne-Sofie C. Ahm [a,*], Christian J. Bjerrum [b], Clara L. Blättler [a], Peter K. Swart [c], John A. Higgins [a]

[a] *Princeton University, Department of Geosciences, Guyot Hall, Princeton, NJ 08544, United States*
[b] *University of Copenhagen, Nordic Center for Earth Evolution, Department of Geoscience and Natural Resource Management, Øster Voldgade 10, DK-1350 Copenhagen K, Denmark*
[c] *Department of Marine Geosciences, Rosenstiel School of Marine and Atmospheric Science, University of Miami, 4600 Rickenbacker Causeway, Miami, FL 33149, United States*

Received 4 August 2017; accepted in revised form 23 February 2018; available online xxxx

Abstract

Shallow-water carbonate sediments constitute one of the most abundant and widely used archives of Earth's surface evolution. One of the main limitations of this archive is the susceptibility of the chemistry of carbonate sediments to post-depositional diagenesis. Here, we develop a numerical model of marine carbonate diagenesis that tracks the elemental and isotopic composition of calcium, magnesium, carbon, oxygen, and strontium, during dissolution of primary carbonates and re-precipitation of secondary carbonate minerals. The model is ground-truthed using measurements of geochemical proxies from sites on and adjacent to the Bahamas platform (Higgins et al., 2018) and authigenic carbonates in the organic-rich deep marine Monterey Formation (Blättler et al., 2015). Observations from these disparate sedimentological and diagenetic settings show broad covariation between bulk sediment calcium and magnesium isotopes that can be explained by varying the extent to which sediments undergo diagenesis in seawater-buffered or sediment-buffered conditions. Model results indicate that the covariation between calcium and magnesium isotopes can provide a semi-quantitative estimate of the extent and style (fluid-buffered vs. sediment-buffered) of early marine diagenesis. When applied to geochemical signatures in ancient carbonate rocks, the model can be used to quantify the impact of early marine diagenesis on other geochemical proxies of interest (e.g. carbon and oxygen isotopes). The increasing recognition of early marine diagenesis as an important phenomenon in shallow-water carbonate sediments makes this approach essential for developing accurate records of the chemical and climatic history of Earth from the chemical and isotopic composition of carbonate sediments.

Keywords: Carbonate diagenesis; Carbonate mineralogy; Ca isotopes; Mg isotopes; Numerical Modeling

1. INTRODUCTION

Marine carbonate sediments are one of the most important archives of Earth's history because they are abundant, span 3 billion years, and have no significant detrital component – generally they are interpreted as being precipitated from cations (Ca^{2+}, Mg^{2+}, Sr^{2+}, etc.) and carbonate ions (CO_3^{2-}) in equilibrium with contemporaneous seawater. The chemical and isotopic composition of carbonate sediments has been widely used to reconstruct the global carbon and oxygen cycles and the history of Earth's surface environment (Broecker, 1970; Knoll et al., 1986; Hayes and Waldbauer, 2006). However, to develop accurate

* Corresponding author.
E-mail address: ascahm@gmail.com (A.-S.C. Ahm).

https://doi.org/10.1016/j.gca.2018.02.042
0016-7037/

records of Earth's past surface environment, it is essential to recognize that all carbonate sediments have experienced some post-depositional diagenetic alteration of their primary chemistry during the transformation from unlithified sediments into rocks (Bathurst, 1976; Swart and Eberli, 2005; Higgins et al., 2018). These diagenetic reactions can alter and in some cases completely reset the primary major, minor, and trace element chemistry of the sediment (Allan and Matthews, 1982; Banner and Hanson, 1990).

The extent to which carbonate diagenesis alters the chemical and isotopic composition of the sediment depends on four features of the diagenetic environment: (1) the composition of the diagenetic fluid, (2) the reactivity of the carbonate minerals over time, (3) the mechanism of solute transport (e.g. diffusion vs. advection), and (4) pressure and temperature. Previous studies of carbonate diagenesis have focused on two particular diagenetic environments: meteoric and deep-burial. Both of these diagenetic regimes leave visible traces of alteration, such as exposure surfaces that can be easily identified in the field or textural changes that can be observed petrographically (Bathurst, 1976; Allan and Matthews, 1982; Dyer et al., 2015). While these regimes are important, they are not the focus of this study. Rather, we are interested in early marine diagenesis associated with the transformation of metastable carbonate polymorphs such as high-Mg calcite and aragonite to diagenetically stabilized low-Mg calcite and dolomite (Malone et al., 2001; Melim et al., 2002; Higgins et al., 2018). Early marine diagenetic alteration, involving seawater or seawater-derived fluids, is widespread in shallow-water marine carbonate sediments and involves mass fluxes between sediments and local pore-fluids that are capable of significantly altering the chemical and isotopic composition of the primary sediment (Fantle and Higgins, 2014; Higgins et al., 2018).

The sensitivity of elements in carbonate sediment to early marine diagenesis is determined, to a first order, by the abundance of the element in seawater-derived pore-fluids compared to bulk carbonate sediment. Carbon-isotope values ($\delta^{13}C$) are regarded as the most diagenetically robust of the geochemical systems, due to the high concentration of carbon in carbonate sediments relative to most diagenetic pore-fluids (Banner and Hanson, 1990; Derry, 2010). It should be noted that remineralization of organic carbon is an important factor (although not considered explicitly in this paper) that may change the sensitivity of $\delta^{13}C$ values to early marine diagenesis by affecting both pore-fluid chemistry and dissolution rates (Patterson and Walter, 1994; Irwin et al., 1977). Other major constituents such as calcium isotopes ($\delta^{44/40}Ca$) in limestone and both calcium and magnesium isotopes ($\delta^{26}Mg$) in dolomite are expected to be similarly or somewhat less resistant to diagenesis than carbon as calcium and magnesium are more abundant than carbon in seawater and seawater-derived fluids. On the other hand, the isotopic composition of oxygen ($\delta^{18}O$), another major constituent in carbonates, is easily reset due to the abundance of oxygen in water (H_2O).

Solute transport is perhaps the second most important variable in many diagenetic systems as it determines, in part, the extent to which diagenesis is dominated by the chemistry of the fluid (fluid-buffered) or the chemistry of the sediment (sediment-buffered). Diagenetic systems where diffusion dominates tend to favor sediment-buffered diagenesis, whereas systems with significant advective fluid-flow tend to favor fluid-buffered conditions. Potential sources of fluid flow include tidal pumping, wave action, geothermal convection, evaporative reflux, and mixing with meteoric water (Simms, 1984; Kaufman, 1994; Kohout, 1977; Hughes et al., 2007). Critically, fluid flow in shallow-water carbonate systems can create diagenetic systems that are capable of altering even the most robust primary chemical and/or isotopic signals (e.g $\delta^{13}C$, $\delta^{44/40}Ca$, Higgins et al., 2018). Compounding the problem, early marine diagenetic alteration is difficult to identify using either petrographic (Grotzinger and Reed, 1983; Melim et al., 2002) or traditional geochemical indicators (e.g. Mn/Sr; Brand and Veizer, 1980). Generally, this style of diagenesis goes unrecognized and undiscussed in studies of the geochemistry of carbonate sediments in the geologic record.

In this study, we develop a numerical model of mineral dissolution and re-precipitation within the pore space of platform and periplatform carbonates. The model quantifies the resetting of $\delta^{44/40}Ca$, $\delta^{26}Mg$, $\delta^{13}C$, and $\delta^{18}O$ in combination with elemental concentrations of Sr during neomorphism (aragonite-to-calcite), recrystallization (calcite-to-calcite), and dolomitization (calcite-to-dolomite). The model is ground-truthed using published measurements of Bahamian carbonates and authigenic carbonates from the Monterey Formation where the boundary conditions, degree of fluid-rock interaction, and composition of seawater are relatively well known (Supko, 1977; Vahrenkamp et al., 1988; Eberli et al., 1997; Ginsburg, 2001; Swart and Eberli, 2005; Blättler et al., 2015; Higgins et al., 2018). Model results provide quantitative constraints on (1) the composition of the primary mineralogical end-member, (2) the diagenetic end-member, and (3) the composition of the diagenetic fluid. Application of this diagenetic model to ancient carbonate sediments with large datasets of calcium, magnesium, carbon, and oxygen isotopes and major/minor element chemistry will lead to more robust records of secular change for a wide range of carbonate-bound geochemical proxies (e.g. $\delta^{7}Li$, $\delta^{11}B$, $\delta^{34}S_{CAS}$, $\delta^{88/86}Sr$, $\delta^{238/235}U$, I/Ca) and more accurate reconstructions of the history of the global carbon and oxygen cycles.

2. METHODS

2.1. Model setup

Building on published modeling efforts (Banner and Hanson, 1990; Fantle and Higgins, 2014; Blättler et al., 2015), we construct a numerical model that simulates early marine diagenesis of carbonate sediments by stoichiometrically recrystallizing aragonite to low-Mg calcite (neomorphism) or aragonite/calcite to dolomite (dolomitization) assuming conservation of mass of carbon in the sediment. The model transforms one carbonate mineral into another through dissolution and re-precipitation reactions that exchange mass between the sediment and the pore-fluid.

Please cite this article in press as: Ahm A. -S. C., et al. Quantifying early marine diagenesis in shallow-water carbonate sediments. *Geochim. Cosmochim. Acta* (2018), https://doi.org/10.1016/j.gca.2018.02.042

Once precipitated the secondary diagenetic mineral, whether low-Mg calcite or dolomite, is assumed to be unreactive and does not undergo further dissolution. The reaction between fluid and sediment is prescribed by a free parameter, the reaction constant (R), that describes dissolution of the original carbonate mineral and re-precipitation of a stoichiometrically defined diagenetic mineral phase (Table 1). This approach expands the widely used framework by Banner and Hanson, 1990 that assumed homogeneous recrystallization, where the entire solid phases reaches equilibrium with the solution at each iterative time step.

The model is constructed as a 1-D system of boxes that represents a column of porous carbonate sediment (Fig. 1). Each box has a constant volume (1 m^3) and porosity (0.5) and the number of boxes in the sediment column can be defined to specify the thickness of the sediment package and the length scale over which diagenesis takes place (Dyer et al., 2017). A fluid with a prescribed composition (modern seawater) is introduced into the uppermost box of the sediment column where it reacts with the surrounding sediment before passing on to the next box at a constant flow rate (u), driven by unidirectional advection. We assume that fluid flow is dominated by advection and do not consider diffusion ($D = 0$). This assumption is based on observations from modern carbonate platforms that suggest massive dolomitization of relatively thick stratigraphic units can occur within a few million years of sedimentation (Henderson et al., 1999; Vahrenkamp et al., 1988, 1991). We test this assumption by comparing the model results to authigenic dolomites in deep-sea sediments where solute transport occurs predominantly by diffusion (see Section 3.3.2, Blättler et al., 2015).

The time-dependent change in the isotopic composition of the bulk sediment (δ_{total}) can be sub-divided into the relative fraction of primary and secondary minerals within the sediment:

$$\frac{\partial M_s \delta_{total}}{\partial t} = \frac{\partial M_{prim}\delta_{prim}}{\partial t} + \frac{\partial M_{sec}\delta_{sec}}{\partial t} = -R(M_{prim}\delta_{prim} - mC_{prim}\delta_{sec}) \quad (1)$$

Table 1
Summary of model notation and baseline conditions for aragonite to low-Mg calcite neomorphism.

Notation	Definition	Value	Reference
α_{Ca}	Ca isotopic fractionation factor for diagenesis	1.000	Fantle and DePaolo (2007) and Jacobson and Holmden (2008)
α_{Mg}	Mg isotopic fractionation factor	0.998	Higgins and Schrag (2010)
α_C	C isotopic fractionation factor	1.001	Romanek et al. (1992)
α_O	O isotopic fractionation factor	1.0330	Böhm et al. (2000), Horita (2014) and Kim and O'Neil (1997)
K_{Sr}	Distribution coefficient for Sr	0.05	Banner, 1995 and Banner and Hanson (1990)
R	Reaction rate constant	10% myr^{-1}	Baker et al., 1982, Higgins et al. (2018), Swart et al. (1987), and Vahrenkamp et al. (1988)
u	Advection rate	10 cm/yr	Henderson et al., 1999 and Kaufman (1994)
m	Stoichiometric scaling factor	element/ C	
M_f	Mass of element in fluid (mmol/kg)	C = 2.4 Ca = 10.6 Sr = 0.09 Mg = 52.8	Modern seawater (Zeebe and Wolf-Gladrow, 2001)
M_s	Mass of element in primary sediment	C = 12% Ca = 39% Sr = 10 000 ppm Mg = 2500 ppm	Based on stoichiometry of aragonite ($CaCO_3$)
δ_f	Isotopic value of fluid	$\delta^{13}C = -2‰$ $\delta^{44}Ca = 0‰$ $\delta^{18}O = -30.5‰$ $\delta^{26}Mg = -0.8‰$	Based on modern seawater and pore-fluid measurements (Kramer et al., 2000; Swart et al., 2001; Higgins et al., 2018)
δ_s	Isotopic value of primary sediment, based on modern Bahamas	$\delta^{13}C = 5‰$ $\delta^{44}Ca = -1.6‰$ $\delta^{18}O = -2‰$ $\delta^{26}Mg = -3.7‰$	(Eberli et al., 1997; Swart and Eberli, 2005; Higgins et al., 2018)
Φ	Porosity	0.5	
V	Box volume	1 m^3	
ρ_s	Density of solid	1.8 g/cm^3	
ρ_f	Density of fluid	1.0125 g/cm^3	
WR	Cumulative fluid-to-rock ratio	10^1–10^6	time (yrs) × Fluid mass flux (kg/yr)/ Sediment mass (kg)
n	Specific box number		

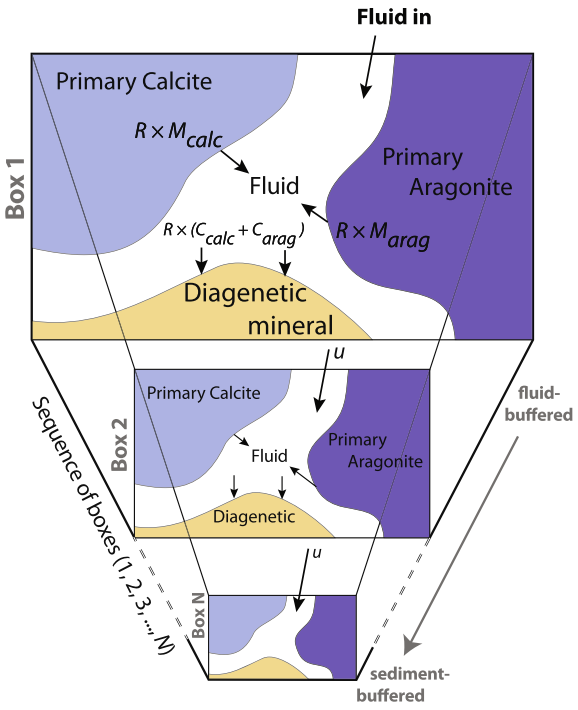

Fig. 1. Schematic setup of the numerical model of carbonate diagenesis. The model consists of a sequence of boxes that represents a column of porous sediments. Boxes are dynamically added or removed to specify the thickness of the sediment column (box 1, 2, 3, . . . , N). Fluid enters the top of the column and flows through the sequence of boxes at a constant advection rate (u), such that the cumulative fluid-to-sediment ratio increases at a similar rate in each box over time (Table 1). Within each box the fluid and sediment react and exchange mass, such that the composition of the fluid evolves continuously along the flow path from box 1 to N following a fluid to sediment-buffered trajectory. Primary carbonates dissolve (calcite and aragonite) at a specific rate defined by the rate constant R. To conserve moles of carbon in the sediment, precipitation of diagenetic minerals (either low-Mg calcite or dolomite) is scaled directly to the dissolution rate of carbon in the primary minerals ($R \times [C_{calc} + C_{arag}]$).

where M_s is the mass of a specific element in the bulk sediment, M_{sec} and δ_{sec} is the mass and isotopic composition in the secondary mineral phase, and M_{prim} and δ_{prim} is the mass and isotopic composition of the primary mineral phase. The isotopic composition of the primary mineral is set to a constant value while the isotopic value of the secondary mineral depends on the pore-fluid chemistry and α, the relevant isotopic fractionation factor ($\delta_{sec} = \delta_{fluid} + 10^3 ln\alpha$). C_{prim} is the mass of carbon in the primary mineral. In order to conserve mass of carbon in the sediment during diagenesis, m is used as a stoichiometric ratio to scale the precipitation rate ($R \times C_{prim} \times m$) of a specific element relative to carbon (e.g. for Mg in dolomite; Mg/C = 0.5).

The continuous dissolution of primary carbonates and precipitation of diagenetic minerals will gradually change the isotopic composition of the fluid (δ_f) along the unidirectional flow path (x), following a fluid- to sediment-buffered trajectory described by the reaction transport equation (modified from Berner, 1980):

$$\frac{\partial M_f \delta_f}{\partial t} = -u \frac{\partial M_f \delta_f}{\partial x} + R[M_{prim}\delta_{prim} - mC_{prim}(\delta_f + 10^3 ln\alpha)] \quad (2)$$

where M_f denotes the mass of a specific element in the fluid within the pore-space of one box (e.g. Ca, Mg, O, C, Sr). When modeling partitioning of non-stoichiometric constituents (trace element partitioning of strontium) we use an elemental distribution coefficient $K_{Sr} \times [Sr/Ca]_{fluid}$ (substituting for mC_{prim}) to describe the incorporation of strontium into the diagenetic sediment.

To solve the reaction transport equation (Eq. (2)), the spatial dimension (∂x) is expressed by finite differences so that the time-dependent differential equation is reduced to an ordinary differential equation that is solved numerically for each box (n):

$$\frac{\partial M_f^n \delta_f^n}{\partial t} = -u \times [M_f^{n-1}\delta_f^{n-1} - M_f^n \delta_f^n] + R(M_{prim}^n \delta_{prim}^n - mC_{prim}^n \delta_{sec}^n) \quad (3)$$

This equation describes the evolution of the fluid composition along a single flow path (from box 1 to N), which controls the composition of the precipitating diagenetic mineral in each box.

Although the conceptual framework of the model is a simplification of the complex geometry of fluid flow in porous carbonate sediments, it can be easily applied to most geochemical and isotopic systems in carbonate sediments. Using the chemistry and isotopic composition of major elements in carbonate sediments (calcium, magnesium, carbon, oxygen, and strontium), the model predicts diagnostic geochemical signatures for diagenesis. This approach can thus be used to evaluate the extent to which all carbonate-bound geochemical proxies have been affected by early marine diagenetic alteration.

A MatLab file with the full model code is available from https://github.com/Anne-SofieAhm/Diagenesis-model

2.2. Model baseline

A set of baseline conditions are used in the model that derive from observations of early marine diagenesis in modern carbonate sediments in the Bahamas (Table 1). The three most important of these are (1) the rate of carbonate recrystallization and/or neomorphism (R), (2) the rate of external fluid flow (u), and (3) the initial chemical and isotopic composition of the diagenetic fluid. Together these variables set the timescale of diagenesis, the range of diagenetic conditions captured by the model, and the chemical and isotopic composition of the final diagenetic mineral. For R, we use 10% Myr^{-1}, a value that is broadly consistent with previous studies of recrystallization, neomorphism, and/or dolomitization in young carbonate sediments in both shallow (Baker et al., 1982; Vahrenkamp et al., 1991; Higgins et al., 2018) and deep-sea settings (Richter and DePaolo, 1987; Fantle and DePaolo, 2006). In particular, measurements of $^{87}Sr/^{86}Sr$ ratios in Neogene dolomites from around the world suggest that early dolomitization can occur in as little as a few million years (Swart et al., 1987; Vahrenkamp et al., 1991, 1988). For u, we use 10

cm/yr, a rate that has been observed in the upper 10's of meters of carbonate sediments on the Bahamas slope from pore-fluid profiles of Cl^- concentrations and U isotopes (Henderson et al., 1999) and estimates from large scale numerical models of fluid flow in carbonate platforms (Kaufman, 1994). The baseline number of boxes (N) in the model is 50, with each box having a volume of 1 m^3 corresponding to a fluid flow path length of 50 m. Sensitivity tests indicate that this length-scale captures the full range of observed diagenetic variability with respect to carbon, calcium, and magnesium.

The initial chemical and isotopic composition of the diagenetic fluid is modern seawater whose carbon-isotope ratios have been influenced by a small degree of respiration of organic carbon, in order to match pore-fluid estimates from the top of cores from the Bahamas transect (i.e. $\delta^{44}Ca = 0‰$, $\delta^{26}Mg = -0.8‰$, $\delta^{18}O = -30.5‰$ (V-PDB), $\delta^{13}C = -2‰$; Eberli et al., 1997; Kramer et al., 2000; Swart et al., 2001; Higgins et al., 2018). For simplicity we neglect additional redox reactions in the subsurface that may modify the chemical and isotopic composition of the fluid. We recognize that these reactions, particularly those associated with respiration of organic carbon with a diverse range of electron acceptors (e.g. O_2, SO_4^{2-}, etc.), may play an important role in determining the chemical and isotopic composition of the diagenetic end-member for some proxies (i.e. $\delta^{13}C$ and any redox sensitive species) and note that the model easily could be adapted to incorporate these effects.

A summary of model notations and variables can be found in Table 1 and sensitivity tests of the model to different boundary conditions can be found in the supplementary material.

2.3. Geochemical data used for model validation

To validate the model we use a range of previously published geochemical measurements from the Bahamas and from the Monterey Formation, in addition to new measurements from San Salvador Island (Supko, 1977; Swart et al., 1987; Vahrenkamp et al., 1991, 1988; Eberli et al., 1997; Ginsburg, 2001; Swart and Eberli, 2005; Blättler et al., 2015; Higgins et al., 2018).

Ca isotope measurements from the Bahamas bank (Higgins et al., 2018) and Monterey Formation (Blättler et al., 2015) are reported as the relative abundance of ^{44}Ca versus ^{40}Ca using standard delta notation, normalized to the isotopic composition of modern seawater (the $\delta^{44/40}Ca$ value for SRM 915a is $-1.86‰$ on the seawater scale, Higgins et al., 2018). Similarly, Mg isotope ratios are expressed as the relative abundance of ^{26}Mg versus ^{24}Mg, normalized to the DSM3 standard (the $\delta^{26}Mg$ value for modern seawater is $-0.83‰$ relative to DSM3, Higgins et al., 2018).

The Bahamas bank and Monterey Formation are ideal natural laboratories for studying early marine diagenesis as they span a range of water depths (~5–650 m) and document a wide range of diagenetic conditions including neomorphism of aragonite/high-Mg calcite to low-Mg calcite, dolomitization (Bahamas), and authigenic carbonate formation (Monterey Formation). Fluid flow plays an important role in early marine diagenesis at these sites. Indeed, estimates for rates of fluid flow and reactivity used in the baseline model are derived from studies of some of the same sites included in our sample suite (e.g. Vahrenkamp et al., 1991, 1988; Eberli et al., 1997; Swart et al., 2001, 1987). Detailed descriptions of the geochemistry, sedimentology, and stratigraphy of each site has been published elsewhere (Supko, 1977; Swart et al., 1987; Vahrenkamp et al., 1988, 1991; Eberli et al., 1997; Ginsburg, 2001; Swart and Eberli, 2005; Blättler et al., 2015; Higgins et al., 2018). Here we present a brief summary and refer the reader to the supplementary material for a more detailed description (see supplementary material 1.0).

Among the samples included in this study are cores from ODP Leg 166 drilled on the western margin of the Great Bahama Bank along a transect from the platform margin into the Straits of Florida (Eberli et al., 1997). Cores Clino and Unda were collected from the shallow platform west of Andros Island and provide the proximal end-member (water depth ~ 10 m) to two cores collected from the deeper waters in the straits of Florida: the intermediate Site 1003 (water depth ~ 480 m) and the more distal Site 1007 (water depth ~ 650 m). These sites exhibit variability in $\delta^{44/40}Ca$, $\delta^{13}C$, $\delta^{26}Mg$, $\delta^{18}O$ values, and Sr/Ca ratios that are both stratigraphically coherent and broadly related to mineralogy and depositional environment. In particular, Sites 1003 and 1007 are characterized by $\delta^{13}C$ values that decline with depth from values as high as +5‰ in the upper 50 m down to +1.5‰ around 200 mbsf, followed by a recovery to values of +2–3‰ at depth (>400 mbsf). Bulk sediment $\delta^{44/40}Ca$ values also vary stratigraphically with low $\delta^{44/40}Ca$ values both near the surface and at depth and a broad ~0.7‰ positive excursion with a maximum between 200 and 400 mbsf. The trends observed for bulk sediment $\delta^{13}C$ and $\delta^{44/40}Ca$ values are also mirrored in both $\delta^{18}O$ values and Sr/Ca ratios: $\delta^{18}O$ values are low (~−1‰) in the top and bottom of the sediment columns with a positive excursion reaching +4‰ around 400 mbsf. Sr/Ca ratios are high in the top of the sediment columns (~10 mmol/mol) and fall to a minimum between 200 and 400 mbsf (~1 mmol/mol) before gradually increasing towards 4 mmol/mol at depth (>400 mbsf).

At slope sites (e.g. Sites 1003 and 1007) neomorphism of aragonite to low-Mg calcite appears to be the dominant diagenetic reaction, whereas dolomitization is much more prevalent at sites in platform interiors. Our sample suite includes shallow water cores from the Little Bahamas Bank (LBB; Walkers Cay Island WCI, Sales Cay Island SCI, Grand Bahama Island GB1, GB2) and San Salvador Island that are extensively dolomitized (Fig. 4). These dolomites are compared to samples of authigenic dolomite from the Monterey Formation, consisting of deep-sea organogenic dolomites and authigenic carbonates that precipitated in shallow sediment pore-fluids against a backdrop of intense anaerobic respiration (Bramlette, 1946; Compton, 1988; Miller, 1995). Although these authigenic carbonates precipitated in an environment where solute transport was likely dominated by diffusion, they exhibit covariation in $\delta^{26}Mg$

and $\delta^{44/40}$Ca values that are consistent with the fluid-buffered and sediment-buffered behavior described in Section 3.1 (Blättler et al., 2015).

3. RESULTS

3.1. Carbonate diagenesis along a fluid flow path: fluid-buffered vs. sediment-buffered

Model results for the various geochemical proxies can be understood in terms of the evolution of fluid chemistry along a flow path and its effects on the chemical composition of the associated diagenetic minerals. Pore-fluids proximal to the fluid source (box 1) are buffered by the chemistry of the infiltrating fluid (fluid-buffered); however, farther down the flow path (e.g. box *N*) recrystallization and neomorphism of the carbonate sediment drives the pore-fluid towards a chemical composition that is dictated by the chemistry of the sediment (sediment-buffered). Thus, in spite of the fact that both box 1 and box *N* have experienced the same cumulative fluid-to-sediment ratio and undergone the same extent of recrystallization, the chemical and isotopic composition of the diagenetic minerals in the two boxes are dramatically different – a consequence of the evolution of fluid chemistry and diagenetic conditions along the flow path. The terms fluid- and sediment-buffered should always be defined with respect to a particular elemental or isotopic system. Unless otherwise noted, we will use fluid-buffered and sediment-buffered to refer to diagenetic conditions with respect to carbon in the sediment. Our choice of carbon reflects its stature as the most diagenetically robust geochemical proxy in carbonate sediments. Although the example discussed here is for the conversion of aragonite to dolomite, a similar set of calculations were performed for the conversion of aragonite to calcite and can be found in the supplementary information (Figs. S4 and S6).

For the fluid-buffered end-member (box 1), the diagenetic conversion of aragonite to a dolomite is accompanied by synchronous changes in all geochemical proxies (δ^{13}C, $\delta^{44/40}$Ca, Sr/Ca, δ^{26}Mg, δ^{18}O: Fig. 2A). These bulk geochemical changes can be understood as simple end-member mixing between primary aragonite and a diagenetic carbonate mineral precipitated from unmodified seawater. The chemical and isotopic composition of this diagenetic carbonate mineral is then dictated by the chemical and isotopic composition of seawater and the relevant isotopic fractionation factors and partition coefficients. For example, above cumulative fluid-to-sediment ratios of $\sim 2 \times 10^4$, bulk sediment δ^{18}O, δ^{26}Mg, and Sr/Ca ratios all reflect the initial composition of the diagenetic fluid (Fig. 2D–F). In contrast, model results illustrate that bulk sediment δ^{13}C and $\delta^{44/40}$Ca values do not quite reach the theoretical fluid-buffered end-member in box 1 (Fig. 2B–C). This offset is a consequence of high carbon and calcium content of the sediment and the rates of recrystallization/-neomorphism ($R = 10\%$/yr) and fluid flow ($u = 10$ cm/yr) used in our baseline model (Table 1). Sensitivity tests demonstrate that higher rates of fluid flow and/or slow rates of recrystallization/neomorphism can drive the δ^{13}C and $\delta^{44/40}$Ca values in box 1 further towards the theoretical fluid-buffered limit (Figs. S7 and S8). The critical point, however, is that the final δ^{13}C and $\delta^{44/40}$Ca values of the

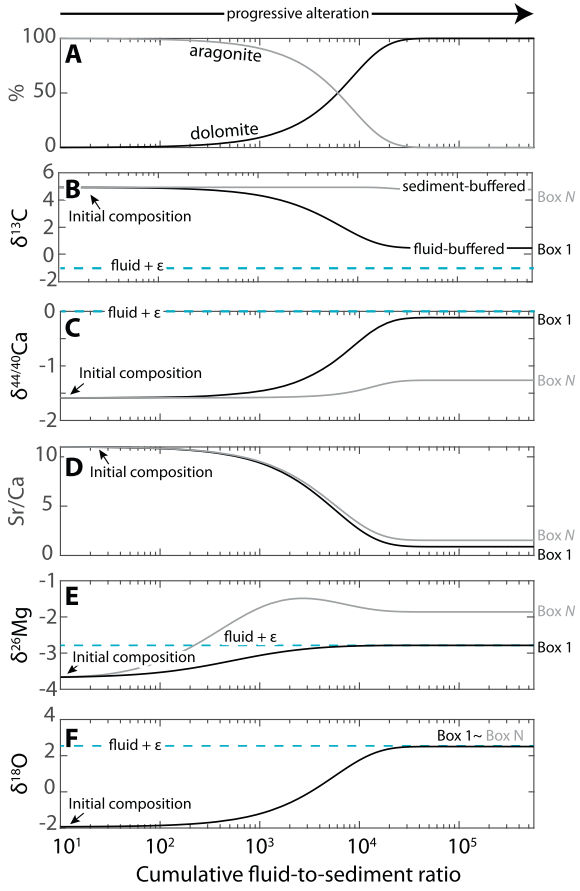

Fig. 2. Schematic of change in bulk sediment chemistry during diagenesis of aragonite to dolomite by interaction with modern seawater. The composition of the bulk sediment evolves at a prescribed reaction rate as fluid flows through the sediment at a constant advection rate (i.e. increasing cumulative mass of fluid relative to the sediment over time; Table 1). The specific geochemical trajectory depends on the length of the flow path (i.e. the specific box number), where box 1 represents the fluid-buffered end-member and box *N* is sediment-buffered with respect to carbon (y-axis). A. Aragonite is altered to dolomite at a prescribed reaction and advection rate (Table 1). (B). Change in bulk sediment δ^{13}C values from an initial composition of aragonite of +5‰ towards the fluid composition of −2‰, accounting for a +1‰ isotopic fractionation during precipitation (ϵ). Note that the primary δ^{13}C values are essentially retained in box *N*. (C). Change in bulk sediment $\delta^{44/40}$Ca values from initial composition of −1.6‰ towards the composition of seawater under fluid-buffered conditions (0‰, $\epsilon = 0$‰). **D.** Change in bulk sediment Sr/Ca ratios (mmol/mol) from high concentrations in primary aragonite to low concentrations in dolomite. **E.** Change in bulk sediment δ^{26}Mg values during dolomitization. Box 1 reaches a value of −2.8‰ reflecting the composition of modern seawater (−0.8‰) accounting for $\epsilon = -2$‰ (Higgins and Schrag, 2010). Box *N* is significantly enriched in ^{26}Mg due to continuous Rayleigh-type distillation of the pore-fluid along the flow path. **F.** Change in bulk sediment δ^{18}O values from an initial composition of −2‰ towards +4‰ (V-PDB) driven by an increase in the fractionation factor during dolomitization at 18 °C (Horita, 2014).

fluid-buffered diagenetic carbonate mineral in the baseline model have been dramatically altered (by ~−4.5‰ and ~+1.5‰, respectively) by early marine diagenesis.

Model results for the sediment-buffered end-member (box *N*) exhibit more complex behaviors with increasing cumulative fluid-to-sediment ratio that differ from proxy to proxy and cannot be simply related to changes in bulk sediment mineralogy (Fig. 2A). For example, bulk sediment $\delta^{13}C$ and $\delta^{44/40}Ca$ values in the sediment-buffered diagenetic end-member are shifted only slightly compared to the initial composition (Fig. 2B and C). In contrast, bulk sediment $\delta^{18}O$ values exhibit very similar behavior in both fluid-buffered and sediment-buffered diagenetic end-members (Fig. 2F). The behavior of bulk sediment $\delta^{26}Mg$ values and Sr/Ca ratios is determined by the relative partitioning and/or stoichiometry of the primary and diagenetic minerals (Fig. 2D and E). During dolomitization, magnesium is strongly partitioned into the diagenetic mineral resulting in a decline in pore-fluid magnesium concentrations along the flow path and an increase in pore-fluid $\delta^{26}Mg$ values (due to Rayleigh-type distillation; Higgins and Schrag, 2010). The result is a sediment-buffered dolomite end-member with elevated $\delta^{26}Mg$ values (Fig. 2E). Bulk sediment Sr/Ca ratios decline precipitously in both fluid-buffered and sediment-buffered end-members, a direct consequence of the large difference in strontium partitioning into aragonite and dolomite. However, the decline is less severe for the sediment-buffered dolomite end-member due to the accumulation of strontium in the pore-fluid along the flow-path (Fig. 2D).

3.2. Geochemical signatures of fluid- and sediment-buffered early marine diagenesis

As cumulative fluid-to-sediment ratios are not independently known for sedimentary carbonates in the rock record, the utility of our diagenetic model lies in its ability to predict relationships between multiple carbonate-bound geochemical proxies that can explain the variability observed in natural datasets (i.e. $\delta^{13}C$, $\delta^{44/40}Ca$, $\delta^{26}Mg$, $\delta^{18}O$, Sr/Ca ratios). This covariation is best illustrated in cross-plots of the various geochemical proxies (i.e. $\delta^{13}C$ vs. $\delta^{44/40}Ca$) where each box (1–*N*) is represented by a point that evolves into a trajectory as recrystallization/neomorphism proceeds in time (i.e. cumulative fluid-to-sediment ratio increases). Together, the boxes/trajectories carve out an area that encompasses all possible combinations of fluid- and sediment-buffered early marine diagenesis for the baseline model (Fig. 3). To the extent that our model is an accurate, if simplified, representation of mass balance during early marine diagenesis, we expect natural sample sets to fall within the modeled area.

Our major-element multi-proxy approach to characterizing early marine diagenesis in shallow-water carbonate sediments offers two major advantages. First, diagenetic alteration of primary $\delta^{13}C$ values is traditionally assessed by comparison with bulk sediment $\delta^{18}O$ isotopes and/or Mn/Sr ratios (Allan and Matthews, 1982; Brand and Veizer, 1980; Derry, 2010). During carbonate diagenesis $\delta^{18}O$ values are expected to be reset in the bulk sediment earlier than $\delta^{13}C$ values resulting in a non-linear relationship between these two isotopic systems (inverted J-curve; Allan and Matthews, 1982; Banner and Hanson, 1990). It is therefore not possible to use the degree of covariation between $\delta^{13}C$ and $\delta^{18}O$ to distinguish resetting in a sediment-buffered vs. a fluid-buffered system with respect to carbon. A similar case can be made for Mn/Sr ratios, as the behavior of strontium during diagenesis is similar to that of $\delta^{18}O$ (Banner and Hanson, 1990), and manganese concentrations in platform carbonates are more influenced by source and dust input than diagenesis (Swart et al., 2014). In contrast, calcium isotopes (and magnesium isotopes in dolomite) are characterized by early marine diagenetic susceptibilities that are similar to carbon, a consequence of the relative abundance of these elements in both the primary and diagenetic sediment compared to unmodified seawater. As a result, the addition of these isotopic systems to the more traditional measurements of $\delta^{18}O$ values and Sr/Ca ratios can be used to identify early marine diagenesis that occurs under both fluid-buffered and sediment-buffered conditions. Second, for each pair of geochemical measurements, the model generates an independent estimate of the extent of recrystallization/neomorphism. Pairs of proxies can thus be checked against one another as each should predict the same extent of reaction for a given sample (Fig. S2). Mismatches between different proxy pairs may indicate incorrect boundary conditions (e.g. the choice of the isotopic fractionation factor or the elemental concentration of the fluid) or later stage burial and/or meteoric diagenesis (especially for Sr/Ca ratios and $\delta^{18}O$ values).

3.2.1. $\delta^{13}C$ vs. $\delta^{44/40}Ca$ values

Early marine diagenesis under both fluid-buffered (box 1) and sediment-buffered (box *N*) conditions produces a diagenetic assemblage characterized by covariation between bulk sediment $\delta^{13}C$ and $\delta^{44/40}Ca$ values (Fig. 3). The sediment-buffered end-member largely retains the high $\delta^{13}C$ and low $\delta^{44/40}Ca$ values of the original aragonite (in spite of the mineralogical change) whereas the fluid-buffered end-member is shifted to lower $\delta^{13}C$ values and higher $\delta^{44/40}Ca$ values. Part of this shift in both $\delta^{13}C$ and $\delta^{44/40}Ca$ values is mineralogical as aragonite is enriched in ^{13}C and ^{40}Ca (Romanek et al., 1992; Gussone et al., 2005). However, differences in the $\delta^{13}C$ of dissolved inorganic carbon (DIC) in seawater and early diagenetic fluids and the rate-dependence of calcium isotope fractionation ($\alpha \sim 1.000$ at rates associated with early marine diagenesis; Fantle and DePaolo, 2007; Jacobson and Holmden, 2008) also play important roles in determining the magnitude of the shift in both $\delta^{13}C$ and $\delta^{44/40}Ca$ values associated with fluid-buffered diagenesis (Fig. 3).

3.2.2. $\delta^{44/40}Ca$ vs. $\delta^{18}O$ values

In contrast to model cross plots involving $\delta^{13}C$ and $\delta^{44/40}Ca$ values, cross-plots of $\delta^{18}O$ vs. $\delta^{44/40}Ca$ values show no covariation in the diagenetic end-member (i.e. $\delta^{18}O$ values are constant for a given % alteration). This behavior reflects the baseline model conditions that generate fluid-buffered conditions for oxygen in the carbonate sediment

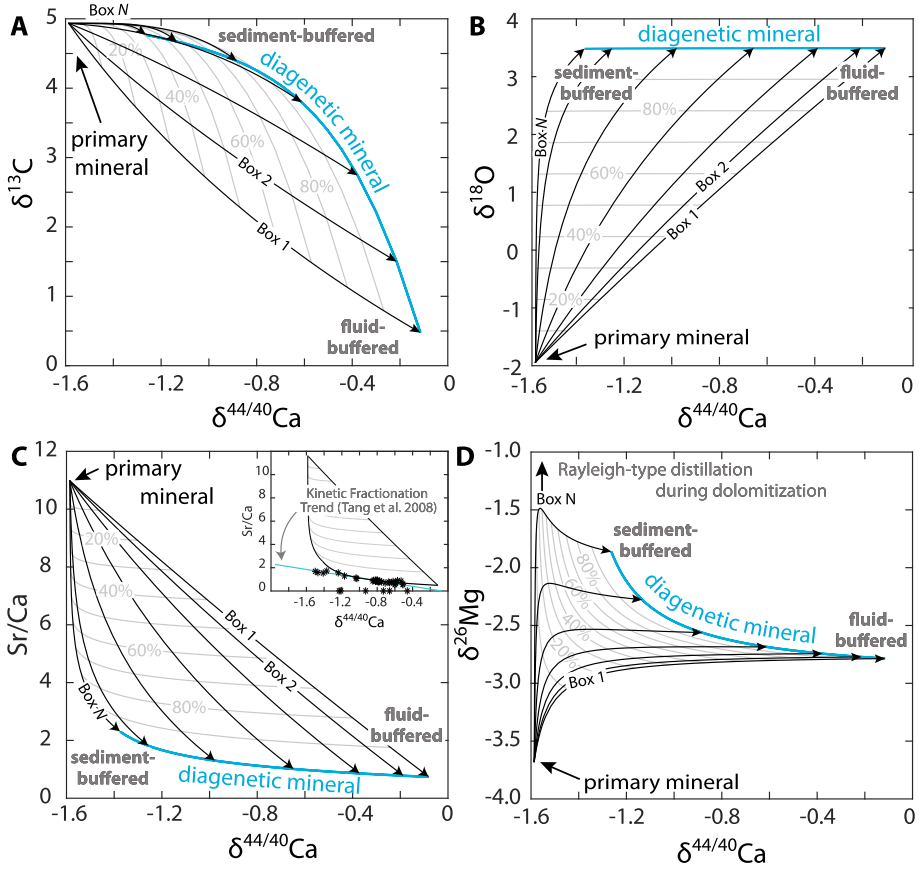

Fig. 3. Schematic illustrating the range of compositions attained by the bulk sediment during dolomitization (A, D) or neomorphism (B, C) of primary aragonite following reaction with modern seawater. Gray lines represent percentiles of the degree of alteration of the bulk sediment (from 0% to 100%). The fully recrystallized sediment is represented by the diagenetic end-member (thick blue line). Each percentile has a fluid- and a sediment-buffered end-member (box 1 to *N*). (A). Modeled trajectories illustrating the correlation between $\delta^{13}C$ and $\delta^{44/40}Ca$ values in the bulk sediment during dolomitization (B). Modeled trajectories illustrating the correlation between $\delta^{18}O$ and $\delta^{44/40}Ca$ values in the bulk sediment during neomorphism. Despite the system being fully sediment-buffered (with respect to Ca) in box *N*, the $\delta^{18}O$ value is consistently reset across all boxes. (C). Modeled trajectories illustrating the correlation between Sr/Ca ratios (in mmol/mol) and $\delta^{44/40}Ca$ values (relative to seawater) in the bulk sediment during neomorphism. For comparison with the model phase-space, the insert in (C) illustrates the predicted rate dependent relationship between Sr/Ca ratios and the fractionation factor of $\delta^{44/40}Ca$ observed from precipitation experiments (Tang et al., 2008). (D). Modeled trajectories illustrating the correlation between $\delta^{26}Mg$ and $\delta^{44/40}Ca$ values during dolomitization.

over the entire length scale (50 m). Increasing the length scale (number of boxes), reducing the reaction rate (R), or decreasing the rate of fluid flow (u), or any combination of the three can produce model results with more sediment-buffered conditions for oxygen isotopes, though the required changes are generally extreme (see supplementary material Section 5). Covariation between bulk sediment $\delta^{18}O$ vs. $\delta^{44/40}Ca$ values does occur in sediments across different stages of % alteration reflecting mixing between primary and diagenetic mineral end-members (trajectory for box 1 in Fig. 3).

3.2.3. $\delta^{44/40}Ca$ values vs. Sr/Ca ratios

Diagenetic carbonate minerals (calcite and dolomite) are generally characterized by low concentrations of Sr (< 1 mmol/mol; Kinsman, 1969; Banner, 1995) in comparison to primary aragonite (Sr/Ca ~ 10 mmol/mol; Kinsman, 1969; Banner, 1995). As a result, the modeled Sr/Ca ratio of the sediment is always lowered during marine diagenesis even when the concentration of Sr^{2+} in the pore-fluid increases (relative to Ca^{2+}) (Banner, 1995; Brand and Veizer, 1980; Fantle and DePaolo, 2006). For our baseline conditions the model predicts that fluid-buffered diagenesis of aragonite results in a significant decrease in the Sr/Ca ratio of the sediment to less than 1 (>90% of initial Sr lost), whereas sediment-buffered diagenesis of aragonite lowers the ratio of Sr/Ca to ~ 1–4 (50–90% of initial Sr lost; Fig. 2D). As expected, the decrease in Sr/Ca ratios in the fluid-buffered end-member (box 1) mirrors the simultaneous increase in $\delta^{44/40}Ca$ values, reflecting the mixing of primary and diagenetic mineral end-members (Fig. 3C). During sediment-buffered diagenesis, however, the bulk sediment retains $\delta^{44/40}Ca$ values of the primary aragonite and Sr/Ca ratios remain relatively high, though still substantially lower than initial Sr/Ca ratios (box *N* in Fig. 3C). In summary, model results indicate that paired measurements of bulk sediment $\delta^{44/40}Ca$ values and Sr/Ca ratios may serve as a geochemical signature for the identifi-

Please cite this article in press as: Ahm A. -S. C., et al. Quantifying early marine diagenesis in shallow-water carbonate sediments. *Geochim. Cosmochim. Acta* (2018), https://doi.org/10.1016/j.gca.2018.02.042

cation of primary aragonite (low $\delta^{44/40}$Ca values and high Sr/Ca ratios) as well as the alteration of this aragonite by fluid-buffered early marine diagenesis (elevated $\delta^{44/40}$Ca values and lower Sr/Ca ratios).

3.2.4. $\delta^{44/40}$Ca vs. δ^{26}Mg values

The magnesium content of dolomite is 10–100 times larger than any potential precursors (aragonite or calcite). As a result, the behavior of pore-fluid δ^{26}Mg values during dolomitization and the δ^{26}Mg values of the dolomite produced depend on relative rates of magnesium supply (by advection or diffusion) and magnesium removal (by dolomite formation). During dolomitization, progressive removal of magnesium from the pore-fluid along the flow path is associated with significant isotopic fractionation ($\alpha = 0.998$) resulting in an increase in the downstream pore-fluid δ^{26}Mg values due to Rayleigh-type distillation (Higgins and Schrag, 2010; Fantle and Higgins, 2014; Blättler et al., 2015). Incorporation of this isotopically distilled pore-fluid magnesium during dolomite precipitation leads to sediment-buffered dolomites that have relatively high and variable δ^{26}Mg values and low $\delta^{44/40}$Ca values, as the calcium in sediment-buffered dolomites is derived mostly from the precursor carbonate mineral (Fig. 3D). In contrast, fluid-buffered dolomites are characterized by low δ^{26}Mg values and high $\delta^{44/40}$Ca values, a consequence of the disparate fractionation factors for magnesium (~0.998 Higgins and Schrag, 2010) and Ca (~0.9998–1.000 Fantle and DePaolo, 2007; Jacobson and Holmden, 2008) in dolomite precipitated from seawater at ambient temperatures and pressures (Fig. 3D).

For baseline model conditions, the slope and range of the covariation between δ^{26}Mg and $\delta^{44/40}$Ca values in the diagenetic end-member dolomite is predominantly controlled by the concentrations and the isotopic composition of magnesium and calcium in the dolomitizing fluid (seawater). Changes in the magnesium and/or calcium isotopic composition of seawater will shift the model cross-plot space accordingly: When the dolomitizing fluid has a higher concentration of calcium relative to magnesium, $\delta^{44/40}$Ca values in the end-member dolomite tend to be more enriched and less variable (fluid-buffered) for a wide range in δ^{26}Mg values, steepening the slope of the covariation between δ^{26}Mg and $\delta^{44/40}$Ca values in the dolomite end-member (Fig. S10). Similarly, when the dolomitizing fluid has a higher concentration of magnesium relative to calcium, δ^{26}Mg values tend to be more negative and span a narrower range (Fig. S11). As a result, the slope of the covariation in the dolomite end-member will decrease, leading to δ^{26}Mg values that are less variable for a wider range in $\delta^{44/40}$Ca values.

3.3. Model validation and case studies

In this section we validate the model by comparison to natural datasets, examining the covariation (or lack thereof) between multiple carbonate-bound geochemical proxies. We use a set of boundary conditions (Table 2), variable extents of diagenetic alteration (i.e. the length of the trajectories in Fig. 3), and location along the flow path (i.e. box 1–*N* in Fig. 3). All of the samples date from the recent geologic past (i.e. the last ~15 Ma) and model boundary conditions for some elements (e.g. concentrations and isotopic compositions of calcium and magnesium in seawater) can be assumed to be similar to modern or reconstructed from independent archives (i.e. $\delta^{44/40}Ca_{fluid}$ from Sites 1003 and 1007 Higgins et al., 2018). Other boundary conditions (e.g. $\delta^{18}O_{fluid}$, $\delta^{13}C_{fluid}$) are determined iteratively by fitting the model to the data (Table 2). We regard the modeling exercise a success if the modeled phase space for each of the pairs of geochemical proxies (e.g. δ^{13}C vs. $\delta^{44/40}$Ca, Sr/Ca vs $\delta^{44/40}$Ca, δ^{18}O vs. $\delta^{44/40}$Ca) captures the variability in the data and is internally consistent; i.e. predicts similar degrees of alteration for each pair of modeled proxy data. In other words, data points that plot on the 80% recrystallization line in a cross-plot of δ^{13}C vs. $\delta^{44/40}$Ca should also sit on the 80% (± 20%) line in a cross-plot of Sr/Ca vs. $\delta^{44/40}$Ca, δ^{18}O vs. $\delta^{44/40}$Ca, etc. (see Fig. S2).

3.3.1. Case study 1: Neomorphism of aragonite on the slope and margin of the Great Bahama Bank (ODP Sites 1003, 1007, and Clino/Unda)

Cross-plots of Sr/Ca ratios vs. $\delta^{44/40}$Ca values, δ^{13}C vs. $\delta^{44/40}$Ca values, and δ^{18}O vs. $\delta^{44/40}$Ca values for samples from the slope and margin of the Great Bahama Bank illustrate significant covariation between these proxies (Fig. 5A–F). There are notable exception with δ^{13}C vs. $\delta^{44/40}$Ca values in older sediments (Miocene to Pliocene) from Sites 1003 and 1007 (Fig. 5D). We suspect that this disagreement (Fig. 5C vs. 5D) is due to a change in the δ^{13}C value of platform aragonite between the Miocene-Pliocene and the Pliocene-Pleistocene and for this reason we model neomorphism separately during these two time periods (Fig. 5A, C, E and B, D, F). The only difference in the model runs for the two time periods is the δ^{13}C value of the end-member primary aragonite (+5‰ for the Pliocene-Pleistocene versus +3.2‰ for the Miocene-Pliocene; Table 2).

The model simulates the complete conversion of platform aragonite to low-Mg calcite using the parameters listed in Table 2. It is worth noting that by fitting the model to the data (Fig. 5), initial $\delta^{44/40}Ca_{fluid}$ values are estimated to −0.5‰ relative to modern seawater. As this model result is non-unique (i.e. a similar model fit could be obtained by decreasing the Ca isotope fractionation factor by −0.5‰), we attribute the estimated difference between modern seawater and model fluid values to (1) uncertainties in the Ca isotopes fractionation factor during early marine diagenesis in shallow water carbonates (~0–0.2‰, Higgins et al., 2018) and (2) a component of horizontal fluid flow bringing isotopically light Ca from carbonate dissolution upstream (evidenced by pore-fluid measurements, Higgins et al., 2018).

The model phase space for boxes 1 to *N* captures, both qualitatively and quantitatively, the covariation in all three pairs of proxy cross-plots (Fig. 5). This agreement suggests that the covariation observed in the data can largely be explained by varying extents of early marine diagenesis of metastable platform carbonate under both fluid-buffered

Table 2
Model boundary conditions for each scenario: (1) Modern early marine diagenesis, 0–400 mbsf (2) Miocene early marine diagenesis, 400–1200 mbsf; (3) Later burial diagenesis, 400–1200 mbsf; (4) Dolomitization in San Salvador and LBB; and (5) authigenic dolomites from the Monterey Formation. The symbol '–' indicates that the parameter was not considered in the specific model scenario. $\delta^{44/40}$Ca values are reported relative to seawater, δ^{26}Mg relative to DSM-3, δ^{13}C relative to V-PDB, and δ^{18}O relative to V-PDB.

Parameter	(1)	(2)	(3)	(4)	(5)
α_{Ca}	1.000	1.000	–	1.0000	1.0000
α_{Mg}	0.998	0.998	–	0.998	0.998
α_{C}	1.001	1.001	–	1.0022	1.0022
α_{O}	1.0324	1.0324	1.0278	1.0335	–
K_{Sr}	0.05	0.05	–	0.01	0.01
R	2% myr^{-1}	2% myr^{-1}	2% myr^{-1}	4% myr^{-1}	8% myr^{-1}
u	10 cm/yr	10 cm/yr	10 cm/yr	10 cm/yr	10 cm/yr
Diagenetic mineralogy	Calcite	Calcite	Calcite	Dolomite	Dolomite
Primary mineralogy	Aragonite	Aragonite	Aragonite	Aragonite	Calcite
M_f (mmol/kg)	Ca: 10.6	10.6	–	10.6	10.6
	Mg: 52.8	52.8	–	52.8	52.8
	C: 2.9	2.9	–	2.9	2.9
	Sr: 0.09	0.09	–	0.09	0.09
δ_f (‰)	$\delta^{44/40}$Ca: −0.5‰	−0.5‰	–	0‰	0‰
	δ^{26}Mg: −0.8‰	−0.8‰	–	−0.8‰	−0.8‰
	δ^{13}C: −2‰	−2‰	–	−2‰	–
	δ^{18}O: −29‰	−29‰	−29‰	−29‰	–
δ_s (‰)	$\delta^{44/40}$Ca: −1.6‰	−1.6‰	–	−1.4‰	−1.1‰
	δ^{26}Mg: −3.8‰	−3.8‰	–	−3.8‰	−3.8‰
	δ^{13}C: 5‰	3.2‰	–	3‰	–
	δ^{18}O: −1.5‰	−1.5	3‰	0‰	–

and sediment-buffered conditions. The model predicts that the Pleistocene-Pliocene samples were neomorphosed during early diagenesis in a more fluid-buffered open-system than the Pliocene-Miocene samples, ranging from 0% to 100% alteration, and suggests that diagenesis in these sediments is ongoing. The majority of the Pliocene-Miocene samples, on the other hand, were not completely neomorphosed during early marine diagenesis (40–85%) but were subsequently buried and instead converted to low-Mg calcite at depth in more sediment-buffered conditions, thereby generally retaining higher Sr/Ca ratios and lower $\delta^{44/40}$Ca values.

The model phase space also captures the covariation between δ^{18}O and $\delta^{44/40}$Ca values in the Pleistocene-Pliocene samples. However, there is no model output for Miocene-Pliocene sediments (Fig. 5F) because we interpret the covariation between δ^{18}O and $\delta^{44/40}$Ca in these data as having a distinct origin from the Pleistocene-Pliocene samples (Fig. 5E): In the younger samples (Fig. 5E) the covariation reflects fluid-buffered neomorphism of aragonite to calcite. The increase in sediment δ^{18}O values is driven primarily by the difference in temperature between the bank-top surface waters and cooler slope environments (~17 °C; Eberli et al., 1997; Murray and Swart, 2017) and is in excellent agreement with modeled Sr/Ca ratios and δ^{13}C values. Although a similar explanation would appear consistent with Miocene-Pliocene sediments given the strong positive covariation between $\delta^{44/40}$Ca and δ^{18}O values, samples with low $\delta^{44/40}$Ca and δ^{18}O values (and high Sr/Ca ratios) in this interval are composed of calcite. As a result, we interpret these samples as reflecting closed system neomorphism of aragonite to calcite during deeper burial. Under this interpretation the low $\delta^{44/40}$Ca values, high(er) Sr/Ca ratios, and δ^{13}C values of +2 to +3‰ are inherited from the pre-cursor aragonite whereas bulk sediment δ^{18}O values will continue to be susceptible to resetting during burial. Bulk sediment δ^{18}O values are therefore interpreted to reflect the greater depths (and higher temperatures) where remaining aragonite undergoes neomorphism to calcite.

3.3.2. Case study 2: Dolomitization in the Bahamas and the Miocene Monterey Formation

Carbonate sediments are extensively dolomitized across the Bahamas platform. These dolomites can be found, among other places, in several shallow cores (20–100 mbsf) from the Little Bahamas Bank (LBB, Vahrenkamp et al., 1988), in a core from San Salvador Island (Supko, 1977; Vahrenkamp et al., 1991), core Unda, and sporadically in core Clino (between 366–378 m and 484–646 m, Ginsburg, 2001; Swart and Eberli, 2005). Most of these dolomites have formed in reaction with relatively unaltered seawater in the shallow subsurface within a few million years after deposition (Swart et al., 1987; Swart et al., 2001; Vahrenkamp et al., 1991). In contrast to the Bahamian platform dolomites, the deep marine siliceous Monterey Formation contains partly dolomitized carbonate beds and nodules formed as early authigenetic concretionary phases with magnesium and calcium supplied from seawater and precursor carbonate minerals (Bramlette, 1946; Miller, 1995; Blättler et al., 2015).

Cross-plots of Sr/Ca, δ^{13}C, δ^{18}O, and δ^{26}Mg vs. $\delta^{44/40}$Ca values for the platform dolomites from the Bahamas generally match the modeled phase space for the conversion of platform aragonite to dolomite using the parameters listed in Table 2 (Fig. 6A, B, C, and E). These results indicate that

dolomitization occurred under predominantly fluid-buffered conditions, although some of the partly dolomitized samples from Clino are characterized by the low $\delta^{44/40}$Ca values that are expected for sediment-buffered conditions (Fig. 6).

Authigenic dolomites from the Monterey Formation agree with the modeled phase space for the conversion of low-Mg calcite to dolomite and exhibit both sediment-buffered and fluid-buffered characteristics as indicated by the extreme variability in dolomite δ^{26}Mg values and $\delta^{44/40}$Ca values that are as high as > -0.4‰ (Fig. 6D). Model results capture the observed covariation between δ^{26}Mg and $\delta^{44/40}$Ca values in both the bulk samples (open symbols) as well as the residual dolomite (colored symbols; Fig. 6D). Although δ^{13}C values are not modeled explicitly for the Monterey dolomites, the covariation between δ^{13}C, δ^{44}Ca, and δ^{26}Mg values indicate that fluid-buffered dolomites are associated with low δ^{13}C values and sediment-buffered dolomites are associated with high δ^{13}C values (Fig. 6D). This trend agrees with depth profiles of pore-fluid $\delta^{13}C_{DIC}$ values in sedimentary systems similar to the Monterey Formation, generally characterized by an initial decline in δ^{13}C values due to the oxidation of organic matter and/or methane followed by an increase in $\delta^{13}C_{DIC}$ values at depth in the zone of methanogenesis (Claypool and Kaplan, 1974; Irwin et al., 1977; Malone et al., 2002). This ordering places the low δ^{13}C pore-fluid related to sulfate reduction/methane oxidation closer to the sediment–water interface, consistent with more fluid-buffered δ^{26}Mg and $\delta^{44/40}$Ca values. Blättler et al. (2015) derived a similar conclusion for the Monterey dolomites by modeling precipitation of authigenic dolomite at shallow depths in the sediment column and the associated diffusion of calcium and magnesium from seawater to the site of dolomite formation. Based on the extremely wide range of δ^{13}C values observed in dolomites (e.g. −20‰ to +20‰) due to biological processes such as anaerobic CH_4 oxidation and methanogenesis (e.g. Kelts and McKenzie, 1984; Malone et al., 2002; Moore et al., 2004), δ^{26}Mg and $\delta^{44/40}$Ca values are likely to be more robust indicators of the diagenetic environment (fluid-buffered vs. sediment-buffered) than the traditional stable isotope ratios of carbon or oxygen. However, the exact model trajectories of the fluid- to sediment-buffered phase space will depend on the δ^{26}Mg and $\delta^{44/40}$Ca values and Mg/Ca ratio of seawater, all of which may have changed over Earth history (see Section 4.3).

4. DISCUSSION

In spite of the widespread recognition that the transformation of unlithified carbonate sediments into limestone and dolomite involves chemical exchange between solid and the local pore-fluid via recrystallization and neomorphism, the effects of this process (diagenesis) are almost always swept aside using qualitative indicators (e.g. petrography and trace element ratios such as Mn/Sr ratios; Brand and Veizer, 1980). Although these metrics succeed in identifying certain types of alteration (e.g. hydrothermal and/or burial diagenesis), recent work by Fantle and Higgins (2014) and Higgins et al. (2018) indicate that more subtle styles of diagenetic alteration – in particular early marine diagenesis in shallow-water environments – can produce large changes in even the most diagenetically resistant geochemical proxies in the bulk sediment (e.g. δ^{13}C and $\delta^{44/40}$Ca values). The model presented here can reproduce the observed covariation in these and other major and minor element proxies through what is essentially mixing between primary metastable carbonate minerals (aragonite and/or high-Mg calcite) and diagenetic carbonates that formed from a continuum of fluid-buffered to sediment-buffered conditions. This result has two important implications for the interpretation of geochemical proxies in ancient shallow-water carbonate sediments (and dolomites in particular). First, it indicates that variations in mineralogy and the style of early marine diagenesis can produce apparent stratigraphic variability in major element proxies (e.g. δ^{13}C values) in carbonate sediments that do not reflect past changes in the chemical and isotopic composition of contemporaneous seawater. Second, our model results suggest that covariation between multiple major and minor element proxies provides a geochemical fingerprint for both identifying and quantifying the effects of early marine diagenesis in ancient limestones and dolomites.

4.1. Interpreting stratigraphic variability in shallow-water carbonate sediments

Model results suggest that much of the stratigraphic variability observed in carbonate Sr/Ca ratios, δ^{13}C, δ^{18}O, $\delta^{44/40}$Ca, and δ^{26}Mg values in both the Bahamas (Fig. 4) and the Monterey Formation (Blättler et al., 2015) can be explained by mineralogy, early marine diagenesis, and secular changes in the chemistry of shallow platform-top seawater and pore-fluids. In neither case is the stratigraphic variability related to global changes in the δ^{13}C of seawater. The observations that inherently local factors can produce stratigraphically coherent variability presents a challenge to traditional interpretations of δ^{13}C variability in ancient shallow-water carbonate sediments using simple models of global carbon isotope mass balance (e.g. $\delta^{13}C_{in} = [1 - f_{org}] \times \delta^{13}C_{carb} + f_{org} \times [\delta^{13}C_{carb} - \epsilon]$; Kump and Arthur, 1999; Rothman et al., 2003).

The existence of similar carbon isotope values and/or excursions from multiple sites around the globe in rocks of approximately the same age is often cited as strong evidence that the δ^{13}C values record global seawater DIC. Although this is necessary, it is not sufficient to demonstrate that these records reflect global seawater DIC; a change in any number of global boundary conditions could produce globally synchronous changes in the local carbonate producing and/or burial environment (e.g. sea-level, atmospheric oxygen, seawater sulfate). Variation in glacial-eustatic sea-level is perhaps the most straightforward example of a process that can drive synchronous local changes in platform environments (Holmden et al., 1998; Swart, 2008; Ahm et al., 2017). For example, sea-level change has been invoked to explain the de-coupling of δ^{13}C values in shallow water carbonate sediments and the global ocean over the Neogene, as more isotopically

Please cite this article in press as: Ahm A. -S. C., et al. Quantifying early marine diagenesis in shallow-water carbonate sediments. *Geochim. Cosmochim. Acta* (2018), https://doi.org/10.1016/j.gca.2018.02.042

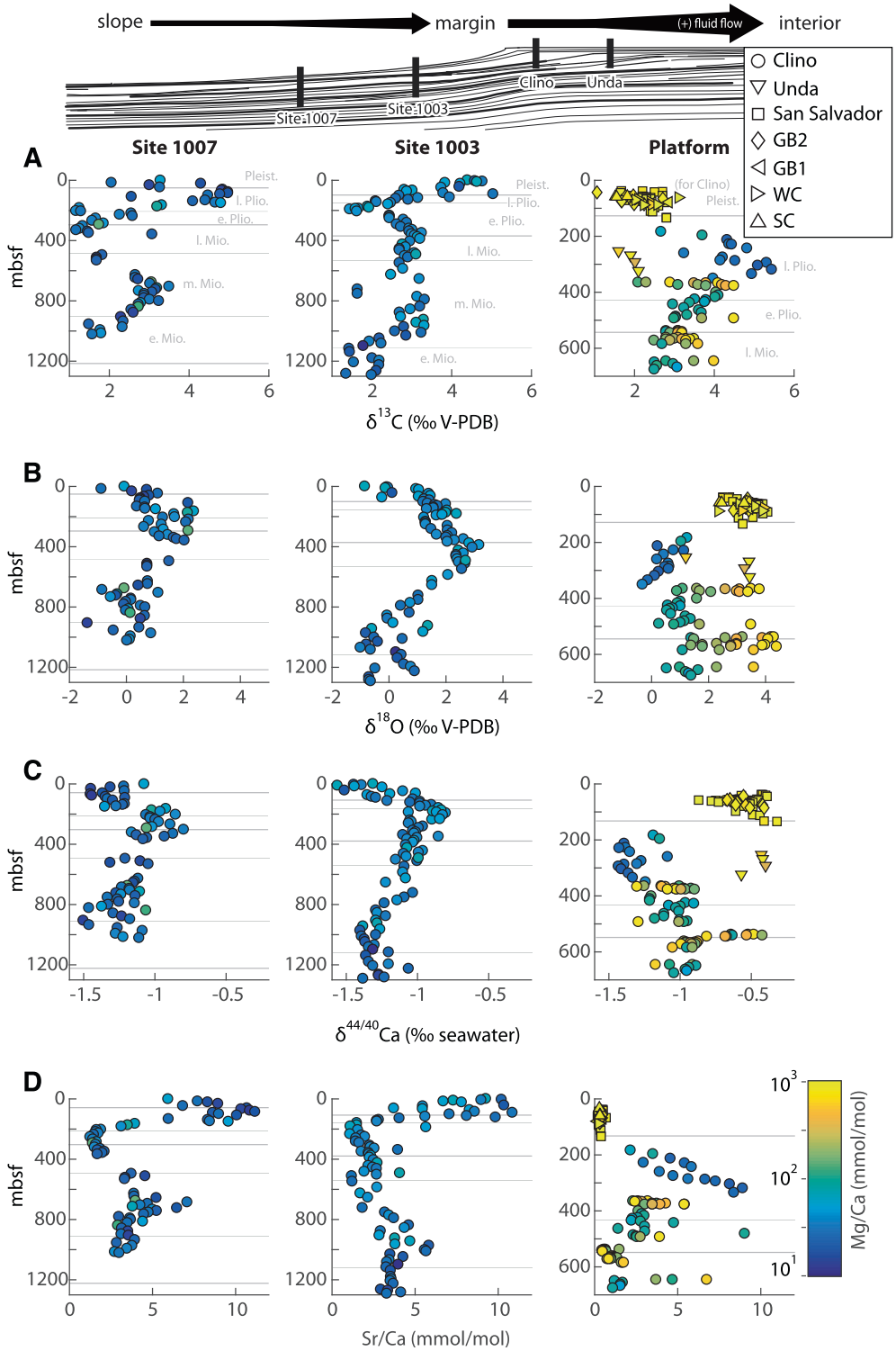

Fig. 4. Published geochemical measurements of (A). $\delta^{13}C$, (B). $\delta^{18}O$, (C). $\delta^{44/40}Ca$, and (D). Sr/Ca ratios (mmol/mol), from the Bahamas Transect: Site 1007, Site 1003, core Clino, core Unda (triangles); a core from San Salvador Island (squares); and four cores from the Little Bahamas Bank (LBB; Walkers Cay Island WC, Sales Cay Island SC, Grand Bahama Island GB1, GB2) (Supko, 1977; Vahrenkamp et al., 1988, 1991; Eberli et al., 1997; Ginsburg, 2001; Swart and Eberli, 2005; Higgins et al., 2018). These cores cover a deep to shallow transect, schematically depicted in the top panel, from the Straits of Florida to the shallow platform and platform interior. Relevant age models are illustrated for Site 1007, Site 1003 and Clino (note that the illustrated platform age model does not apply to core Unda, San Salavador, GB1, GB2, WC, and SC) (Eberli et al., 1997; Ginsburg, 2001).

enriched aragonite is only produced when platforms are flooded during high-stands (Swart and Eberli, 2005; Swart, 2008). This same process can drive synchronous local changes in the intensity of early marine diagenesis in shallow-water environments, as seawater migrates through the platform in response to gradients in hydraulic head created by sea-level variations (Kohout, 1977; Simms, 1984; Kaufman, 1994).

In earlier periods of Earth history there are other global boundary conditions that could have produced dramatic local changes in the chemistry of shallow-water carbonate producing environments. The most likely candidates are the chemical composition of the ocean and atmosphere and biological evolution. Changes in atmospheric oxygen and seawater sulfate are attractive chemical candidates because the abundance of these electron acceptors likely plays an important role in determining both the intensity and spatial distribution of organic carbon and methane cycling in shallow marine environments (Moore et al., 2004; Hayes and Waldbauer, 2006). For example, in the Ediacaran an increase in seawater sulfate concentrations has been suggested to drive widespread transitions in local pore-fluid chemistry and authigenesis, explaining the globally recorded Shuram-Wonoka carbon-isotope excursion as a synchronous diagenetic event (Cui et al., 2017).

4.2. Geochemical fingerprints of mineralogy and early marine diagenesis in limestone and dolomite

Cross-plots of $\delta^{44/40}$Ca, δ^{13}C, δ^{26}Mg, δ^{18}O, and Sr/Ca ratios provide the most reliable means for fingerprinting the effects of mineralogy and early marine diagenesis. We find that of these cross-plots, Sr/Ca ratios versus $\delta^{44/40}$Ca values are likely to provide the best indication of primary aragonite, as a negative correlation between the two is a general prediction of all model results where aragonite is the primary mineral (lower $\delta^{44/40}$Ca values associated with higher Sr/Ca ratios).

The covariation between $\delta^{44/40}$Ca values and Sr/Ca ratios in ancient limestones has been previously cited as evidence for rate-dependent calcium isotope fractionation (Tang et al., 2008; Farkaš et al., 2016). However, our model results suggest that a similar slope is expected for early marine diagenesis of primary aragonite, suggesting that covariation between the two is not a unique indicator of rate-dependence (Fig. 3C). In fact, given independent geochemical and petrographic evidence for primary aragonite throughout the geologic record (e.g. Husson et al., 2015; Kimmig and Holmden, 2017) we regard early diagenetic alteration of aragonite as a better null hypothesis for the observed covariation between Sr/Ca ratios and $\delta^{44/40}$Ca values in ancient limestones.

We are currently aware of five published examples of covariation between carbonate sediment Sr/Ca ratios and $\delta^{44/40}$Ca values, all of which coincide with large carbon isotope excursions, both positive and negative (Fig. 7): Hirnantian limestones from the Monitor Range in N. America (Holmden et al., 2012; Kimmig and Holmden, 2017), Ediacaran limestones and dolomites from the Wonoka Formation in Australia (Husson et al., 2015), Silurian mid-Ludfordian limestones from the Prague basin in the Czech Republic (Farkaš et al., 2016), Triassic-Jurassic boundary limestones from northern Italy (Jost et al., 2017), and Permian–Triassic limestones from China and Turkey (Lau et al., 2017). In each of these examples, cross-plots of Sr/Ca ratios with $\delta^{44/40}$Ca values show a strong resemblance to the data from the Bahamas and generally fall within the model space for the conversion of aragonite to low-Mg calcite and/or dolomite, although the predicted aragonite end-member does not have the same $\delta^{44/40}$Ca value in all cases (e.g. $\delta^{44/40}$Ca down to ~−2‰ in Husson et al. (2015) but only ~−1.65 in Holmden et al. (2012) and Farkaš et al. (2016); Fig. 7). A detailed comparison of these datasets is beyond the scope of this manuscript, but the first-order observation is that the covariation is similar and evokes the early diagenetic conversion of aragonite to low-Mg calcite and dolomite. Although this explanation for the covariation between $\delta^{44/40}$Ca values and Sr/Ca ratios does not provide a mechanistic explanation for the covariation (or lack thereof) between $\delta^{44/40}$Ca values and δ^{13}C values in carbonate sediments during these events, it is strong evidence that the variability in these proxies is associated with local changes in the chemistry of platform-top seawater and variable styles of early marine diagenesis.

The pairing of extreme δ^{13}C values in ancient carbonate rocks (positive and negative) with independent geochemical indicators of former aragonite suggests these values are primary (i.e. primary aragonite neomorphosed under sediment-buffered conditions: Fig. 7B) and likely to be derived from the local DIC reservoir – whether that be on the platform/ramp environment or in an epeiric sea. Carbonate platform environments and epeiric seas have long residence times for surface waters (100's of days: Broecker and Takahashi, 1966; Panchuk et al., 2005). In the modern Bahamas, platform environments are characterized by $\delta^{13}C_{DIC}$ values that are up to ~2‰ higher than open ocean

Table 3
Carbonate based isotope proxies listed in order of approximate sensitivity to early marine diagenesis based on their relative abundance in aragonite in comparison to modern seawater (*these elements are redox sensitive and the partitioning into the carbonate lattice during diagenesis will in addition be affected by the redox state of the pore-waters).

Proxy
δ^{13}C
$\delta^{88/86}$Sr and ^{87}Sr/^{86}Sr
$\delta^{44/40}$Ca
$\delta^{238/235}$U*
δ^{52}Cr*
δ^{56}Fe*
δ^{7}Li
δ^{26}Mg
δ^{11}B
$\delta^{34}S_{CAS}$*
δ^{18}O

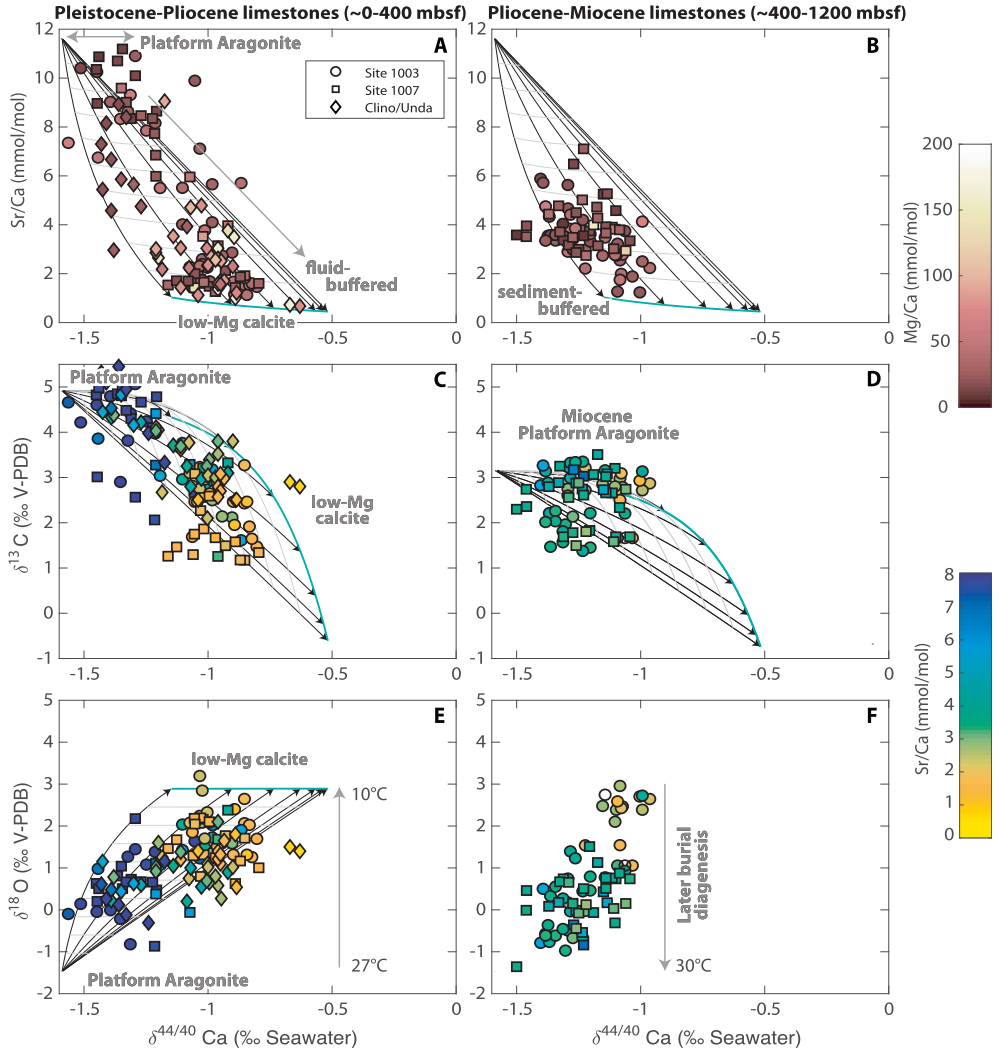

Fig. 5. Modeling results of aragonite to low-Mg calcite neomorphism (Table 2) in comparison with previously published measurements of limestones from Sites 1003, 1007 and core Clino (Higgins et al., 2018). (A). Sr/Ca ratios versus $\delta^{44/40}$Ca values in limestones from the upper 400 mbsf reflecting ongoing neomorphism of aragonite to low-Mg calcite. (B). In limestones from 400 to 1200 mbsf aragonite is neomorphosed to low-Mg calcite during sediment-buffered diagenesis and partly retains its high Sr/Ca ratios and depleted $\delta^{44/40}$Ca values. (C). Model results predict that the covariation between δ^{13}C and $\delta^{44/40}$Ca values in the upper 400 mbsf reflects neomorphism of ^{13}C enriched platform aragonite (+5‰) in reaction with seawater (approaching 0‰). (D). δ^{13}C versus $\delta^{44/40}$Ca values from 400 to 1200 mbsf reflect sediment-buffered diagenesis of Pliocene-Miocene platform aragonite, that has partly retained its primary isotopic signature. (E). Model results predict that the covariation between δ^{18}O and $\delta^{44/40}$Ca values in the upper 400 mbsf reflects mixing between primary aragonite precipitated in the warm platform waters (~27°) and low-Mg calcite formed during early marine diagenesis in the deeper waters (~10°; Eberli et al., 1997). (F). The covariation between δ^{18}O and $\delta^{44/40}$Ca values in the deeper part of the core (400–1200 mbsf) reflects later burial diagenesis with increasing temperature and sediment-buffered conditions.

seawater. The δ^{13}C values of platform-top aragonite sediments in the Bahamas are thus decoupled from the open ocean, recording values of +4 to +5‰ (Swart and Eberli, 2005). Similarly, anomalously high or low δ^{13}C values recorded in ancient carbonate rocks may be generated by variability in the local $\delta^{13}C_{DIC}$ reservoir (Swart, 2008). Potential mechanisms include intense photosynthesis and associated hypercalcification (Farkaš et al., 2016; Holmden et al., 2012), methanogenesis accompanied by methane escape (Hayes and Waldbauer, 2006), kinetic isotope effects associated with CO_2(g) hydration or degassing coupled to intense local primary production (Lazar and Erez, 1992; Stiller et al., 1985), and respiration of terrestrial organic matter (Patterson and Walter, 1994). A possible interpretation of the covariation between large carbon isotope excursions and negative excursions in sediment $\delta^{44/40}$Ca values is that they largely reflect changes in the $\delta^{13}C_{DIC}$ in shallow-water aragonite producing environments (and the style of subsequent diagenetic alteration of that aragonite on platform margins, ramps, and slopes) and not changes in the δ^{13}C values of global seawater DIC.

Please cite this article in press as: Ahm A. -S. C., et al. Quantifying early marine diagenesis in shallow-water carbonate sediments. *Geochim. Cosmochim. Acta* (2018), https://doi.org/10.1016/j.gca.2018.02.042

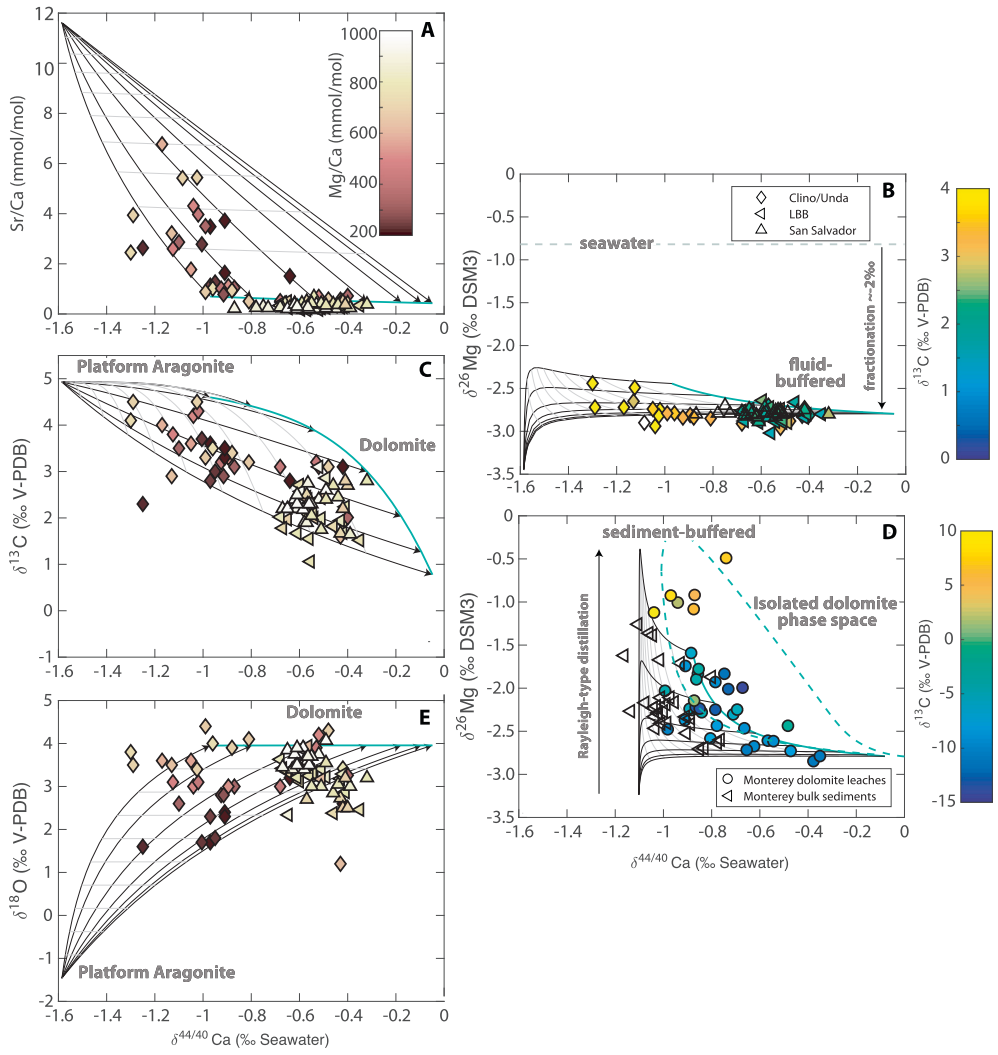

Fig. 6. Modeling results of dolomitization of platform aragonite (Table 2) compared with published measurements of dolomites from the Bahamas and authigenic dolomites from the deep marine Monterey Formation (Blättler et al., 2015; Higgins et al., 2018). (A). Sr/Ca ratios versus $\delta^{44/40}$Ca values in platform dolomites (triangles) and dolomite leaches from core Clino (diamonds). (B). The model predicts that the covariation between δ^{26}Mg and $\delta^{44/40}$Ca values in the Bahamian dolomites reflects fluid-buffered dolomitization in reaction with seawater. (C). Covariation between δ^{13}C and $\delta^{44/40}$Ca values reflecting mixing between aragonite and dolomite in the leaches from core Clino. (D). The model predicts that the covariation between δ^{26}Mg and $\delta^{44/40}$Ca values in the authigenic dolomites from the deep marine Monterey Formation reflects sediment-buffered dolomitization/authigenesis. The blue dashed line encompasses the model phase space for the isolated dolomite component whereas the black arrows represent the composition of the bulk sediment. **E.** Model results of the covariation between δ^{18}O and $\delta^{44/40}$Ca values reflecting mixing between primary aragonite and dolomites formed during early marine diagenesis with a larger δ^{18}O fractionation factor (~1.0335 at 22 °C; Horita, 2014). (For interpretation of the references to color in this figure legend, the reader is referred to the web version of this article.)

4.3. Early diagenetic dolomites as archives of ancient seawater chemistry

The abundance of magnesium and calcium in dolomite makes this paired isotopic system particularly useful for characterizing both the early diagenetic environment where dolomitization occurred (fluid-buffered or sediment-buffered) and the chemical and isotopic composition of the dolomitizing fluid. The modeling results further suggest the range and extent of covariation between δ^{26}Mg and $\delta^{44/40}$Ca values in dolomites may serve as a foundation for the interpretation of a wide range of carbonate-bound proxies (Table 3). One potential obstacle to this approach, however, is that the timing of dolomitization is often poorly known and the identification of early diagenetic dolomite based on field observations, cement textures, or in some cases strontium isotopes is non-unique (Vahrenkamp et al., 1991; Swart et al., 2000). Early diagenetic dolomites are, however, relatively resistant to further diagenetic alteration (Kah, 2000; Geske et al., 2012; Hu et al., 2017) and thus may, counterintuitively, prove to be a more reliable archive of paleoenvironmental information than limestones that have undergone only partial diagenetic stabilization during shallow burial (Higgins et al., 2018).

Please cite this article in press as: Ahm A. -S. C., et al. Quantifying early marine diagenesis in shallow-water carbonate sediments. *Geochim. Cosmochim. Acta* (2018), https://doi.org/10.1016/j.gca.2018.02.042

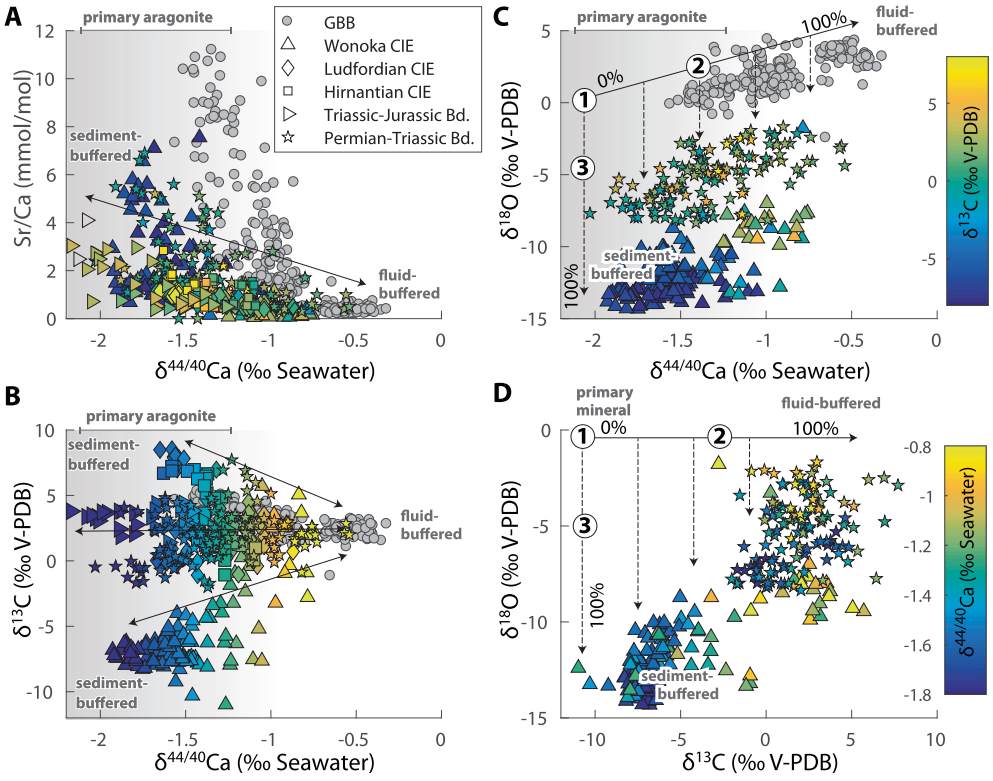

Fig. 7. Cross-plots illustrating the covariation between (A). Sr/Ca ratios and $\delta^{44/40}$Ca values, (B). δ^{13}C and $\delta^{44/40}$Ca values, (C). δ^{18}O and $\delta^{44/40}$Ca values and (D). δ^{18}O and δ^{13}C values in multiple sections containing extreme carbon-isotope excursions (Holmden et al., 2012; Husson et al., 2015; Farkaš et al., 2016; Kimmig and Holmden, 2017; Jost et al., 2017; Lau et al., 2017). The anomalous δ^{13}C values, both positive and negative, consistently coincide with depleted $\delta^{44/40}$Ca values and high Sr/Ca ratios indicating a primary aragonitic origin (gray shaded area), where the isotopic signatures of δ^{13}C and $\delta^{44/40}$Ca are preserved during sediment-buffered diagenesis. Covariation between δ^{18}O and $\delta^{44/40}$Ca values in C and δ^{13}C values in D is attributed to the extent (% alteration) to which primary aragonite (label 1), is recrystallized/stabilized during early seawater-buffered diagenesis (arrow 2). Later stage sediment-buffered alteration under higher temperatures (arrow 3) will to a higher degree reset bulk sediment δ^{18}O values in sediments that were not stabilized during early diagenesis while retain their $\delta^{44/40}$Ca and δ^{13}C values.

As discussed in Section 3.3.2, both the shape and position of the model phase space associated with dolomitization in cross-plots of δ^{26}Mg versus $\delta^{44/40}$Ca values will depend on the Mg/Ca ratio, δ^{26}Mg, and $\delta^{44/40}$Ca values of the dolomitizing fluid. Not every dolomite body is expected to express paired isotopic relationships across the entire phase space but if the phase space is well-defined by sufficient data, it may be possible to use the isotopic covariation to infer the δ^{26}Mg, $\delta^{44/40}$Ca, and Mg/Ca values of ancient seawater. Given uncertainties associated with the fractionation factor of calcium isotopes in shallow-water environments, the δ^{26}Mg value of ancient seawater is likely to be the property most accurately defined by this approach, followed by the $\delta^{44/40}$Ca value and Mg/Ca ratio. In fact, measurements of magnesium isotopes in ancient dolomites are already being used to reconstruct the δ^{26}Mg value of seawater in the past (Hu et al., 2017). However, we note that δ^{26}Mg values can vary by >2‰ within a single dolomite unit (Fig. 6) and that without additional geochemical constraints (e.g. paired $\delta^{44/40}$Ca values) environmental reconstructions based only on δ^{26}Mg values may not be accurate.

4.4. A mineralogical-diagenetic explanation for covariation between δ^{13}C and δ^{18}O values in carbonate sediments

Strong covariation between carbonate δ^{13}C and δ^{18}O values has been observed in many sections of the Ediacaran Shuram-Wonoka carbon-isotope excursion (Fig. 7D). This phenomenon has been attributed to diagenetic alteration by meteroric fluids and/or basinal brines rather than a primary depositional process (Derry, 2010; Knauth and Kennedy, 2009; Swart and Kennedy, 2012). We propose an alternative mechanism that is analogous to the mechanism proposed for the covariation between $\delta^{44/40}$Ca and δ^{18}O values in the Miocene-Pliocene aged samples from the Bahamas (Fig. 5F). We hypothesize that the covariation between δ^{13}C and δ^{18}O values results from differences in the extent to which the original primary aragonite is converted to low-Mg calcite or dolomite during early marine diagenesis. During early marine diagenesis some or all of the metastable carbonate minerals are neomorphosed and/or recrystallized (arrow 2 in Fig. 7C-D), inheriting the δ^{13}C and δ^{18}O values associated with these early diagenetic fluids (and likely preserving them during later burial, Kah, 2000; Geske et al., 2012). In cases

Please cite this article in press as: Ahm A. -S. C., et al. Quantifying early marine diagenesis in shallow-water carbonate sediments. *Geochim. Cosmochim. Acta* (2018), https://doi.org/10.1016/j.gca.2018.02.042

where not all of the carbonate sediment undergoes neomorphism and/or recrystallization in an early diagenetic environment, further burial will eventually lead to recrystallization and neomorphism, likely under more closed system conditions and higher temperatures (leading to resetting of $\delta^{18}O$ values while preserving $\delta^{13}C$ and $\delta^{44/40}Ca$ values, arrow 3 in Fig. 7C and D). The covariation between $\delta^{13}C$ and $\delta^{18}O$ values can thus be understood as the consequence of mixtures of carbonates diagenetically stabilized under fluid buffered conditions and low temperatures with carbonates diagenetically stabilized under sediment-buffered conditions at elevated temperatures.

The explanation for covariation between $\delta^{13}C$ and $\delta^{18}O$ values is consistent with the observed covariation in Miocene-Pliocene samples from Sites 1003 and 1007 in the Bahamas (Fig. 5F), and can be extended to Ediacaran Wonoka Formation where sediment $\delta^{18}O$ values covary with both $\delta^{13}C$ and $\delta^{44/40}Ca$ values during the recovery phase of the calcium isotope excursion (Fig. 7; Husson et al., 2015). In these carbonate rocks, negative $\delta^{44/40}Ca$ values are preserved due to neomorphism of aragonite in predominantly sediment-buffered conditions during late burial diagenesis (lower % alteration during early diagenesis), giving rise to very negative $\delta^{18}O$ values. In contrast, carbonate rocks containing more positive $\delta^{44/40}Ca$ values were likely neomorphosed and stabilized during early marine fluid-buffered diagenesis, thereby preserving more positive $\delta^{18}O$ values (higher % alteration during early diagenesis). Similar covariation is also observed between $\delta^{44/40}Ca$ and $\delta^{18}O$ values in sedimentary carbonates from the Permian-Triassic boundary, suggesting that this phenomena is widespread in the geological record.

5. CONCLUSION

We have built a numerical model that simulates carbonate dissolution and re-precipitation within the pore space. The model quantifies the effects of early marine diagenesis by tracking the elemental and isotopic composition of Ca, Mg, C, O, and Sr/Ca ratios. Model results demonstrate how the evolution of the diagenetic fluid along a single vertical flow-path governs the degree of fluid- versus sediment-buffered diagenesis, and ultimately dictates the degree of diagenetic alteration of several primary isotopic signals.

The model was used to explore the range of isotopic arrays (e.g. $\delta^{44/40}Ca$ versus $\delta^{26}Mg$) that may be generated during early marine diagenesis. These modeled trajectories were ground-truthed against published measurements from sites on the bank top and slope of the Bahamas carbonate platform (Eberli et al., 1997; Higgins et al., 2018; Swart and Eberli, 2005). To reproduce the observed increase in $\delta^{44/40}Ca$ values and decline in aragonite abundance and Sr concentrations, model results require extensive fluid-buffered diagenesis (by modern seawater) in the upper ~0–400 m of the sediment column. In the deeper Miocene part of the cores, model results favor increasingly sediment-buffered diagenesis, identified by depleted $\delta^{44/40}Ca$ values and high Sr/Ca ratios, indicating that the geochemistry is largely inherited from the precursor sediment in spite of the loss of aragonite. These results suggest that fluid flow in the Bahamas platform has evolved over time in concert with changing platform morphology and glacio-eustatic sea-level change.

The model was further tested on a range of shallow-water dolomites across the Bahamas platform and authigenic dolomites from the Monterey Formation (Blättler et al., 2015; Higgins et al., 2018). The results demonstrate that the degree of covariation between $\delta^{44/40}Ca$ and $\delta^{26}Mg$ values can be used to identify fluid-buffered dolomitization (enriched $\delta^{44/40}Ca$ and depleted $\delta^{26}Mg$ values) versus sediment-buffered dolomitization, where Mg has been distilled along the fluid flow path (depleted $\delta^{44/40}Ca$ and enriched $\delta^{26}Mg$ values). In addition, the curvature of the isotopic array contains clues about the relative Mg/Ca ratio of the dolomitizing fluid, providing potential information on past seawater chemistry. By modeling the isotopic arrays against $\delta^{44/40}Ca$ values, $\delta^{26}Mg$ values, and Sr/Ca ratios, we can provide quantitative and robust constraints on the degree of diagenetic alteration and the composition and origin of diagenetic fluids. This modeling approach can be used to see through diagenesis and provide constraints on the chemistry and climatic history of ancient Earth.

ACKNOWLEDGMENTS

A-SCA acknowledges support from The Carlsberg Foundation. This work was supported by the Danish National Research Foundation (Grant No. DNRF53) and by a grant from the Simons Foundation (SCOL 339006 to CLB). JAH acknowledges support from NSF Grant No. IES1410317 and NSF OCE CAREER Grant No. 1654571. We would like to thank Elizabeth Lundstrom for invaluable laboratory assistance. We are grateful for the careful and constructive comments on an earlier version of the manuscript provided by David S. Jones, Emily C. Pope, and Alexandra V. Turchyn.

APPENDIX A. SUPPLEMENTARY MATERIAL

Supplementary data associated with this article can be found, in the online version, at https://doi.org/10.1016/j.gca.2018.02.042.

REFERENCES

Ahm A. S. C., Bjerrum C. J. and Hammarlund E. U. (2017) Disentangling the record of diagenesis, local redox conditions, and global seawater chemistry during the latest Ordovician glaciation. *Earth Planet. Sci. Lett.* **459**, 145–156. https://doi.org/10.1016/j.epsl.2016.09.049.

Allan J. R. and Matthews R. K. (1982) Isotope signatures associated with early meteoric diagenesis. *Sedimentology* **29**, 797–817. https://doi.org/10.1111/j.1365-3091.1982.tb00085.x.

Baker P. A., Gieskes J. M. and Elderfield H. (1982) Diagenesis of carbonates in deep-sea sediment – evidence from Sr/Ca ratios and interstitial dissolved Sr^{2+} data. *J. Sediment. Res.* **52**, 71–82.

Banner J. L. (1995) Application of the trace element and isotope geochemistry of strontium to studies of carbonate diagenesis. *Sedimentology* **42**, 805–824. https://doi.org/10.1111/j.1365-3091.1995.tb00410.x.

Banner J. L. and Hanson G. N. (1990) Calculation of simultaneous isotopic and trace element variations during water-rock interaction with applications to carbonate diagenesis. *Geochim.*

Cosmochim. Acta **54**, 3123–3137. https://doi.org/10.1016/0016-7037(90)90128-8.

Bathurst R. G. C. (1976) Carbonate Sediments and their Diagenesis. *second ed.*. Elsevier Publishing, Amsterdam, The Netherlands.

Berner R. A. (1980) Early Diagenesis. A Theoretical Approach. Earth Surface Processes and Landforms, vol. 7. Princeton University Press. https://doi.org/10.1002/esp.3290070212.

Blättler C. L., Miller N. R. and Higgins J. A. (2015) Mg and Ca isotope signatures of authigenic dolomite in siliceous deep-sea sediments. *Earth Planet. Sci. Lett.* **419**, 32–42. https://doi.org/10.1016/j.epsl.2015.03.006.

Böhm F., Joachimski M. M., Dullo W. C., Eisenhauer A., Lehnert H., Reitner J. and Wörheide G. (2000) Oxygen isotope fractionation in marine aragonite of coralline sponges. *Geochim. et Cosmochim. Acta* **64**, 1695–1703. https://doi.org/10.1016/S0016-7037(99)00408-1.

Bramlette M. N. (1946). The Monterey Formation of California and the Origin of Its Siliceous Rocks, Geological Survey Professional Paper, vol. 212. US Government Printing Office.

Brand U. and Veizer J. (1980) Chemical diagenesis of a multicomponent carbonate system 1: Trace elements. *J. Sediment. Petrol.* **50**, 1219–1236.

Broecker W. S. (1970) A boundary condition on the evolution of atmospheric oxygen. *J. Geophys. Res.* **75**, 3553–3557. https://doi.org/10.1029/JC075i018p03553.

Broecker W. S. and Takahashi T. (1966) Calcium carbonate precipitation on the Bahama Banks. *J. Geophys. Res.* **71**, 1575–1602. https://doi.org/10.1029/JZ071i006p01575.

Claypool G. E. and Kaplan I. R. (1974) *The Origin and Distribution of Methane in Marine Sediments* Marine Science, vol. 3. Springer, US, Boston, MA, pp. 99–139. Marine Science. https://doi.org/10.1007/978-1-4684-2757-8_8.

Compton J. S. (1988) Degree of supersaturation and precipitation of organogenic dolomite. *Geology* **16**, 318–321.

Cui H., Kaufman A. J., Xiao S., Zhou C. and Liu X. M. (2017) Was the Ediacaran Shuram Excursion a globally synchronized early diagenetic event? Insights from methane-derived authigenic carbonates in the uppermost Doushantuo Formation, South China. *Chem. Geol.* **450**, 59–80. https://doi.org/10.1016/j.chemgeo.2016.12.010.

Derry L. A. (2010) A burial diagenesis origin for the Ediacaran Shuram–Wonoka carbon isotope anomaly. *Earth Planet. Sci. Lett.* **294**, 152–162. https://doi.org/10.1016/j.epsl.2010.03.022.

Dyer B., Higgins J. A. and Maloof A. C. (2017) A probabilistic analysis of meteorically altered $\delta^{13}C$ chemostratigraphy from late Paleozoic ice age carbonate platforms. *Geology* **45**(2), 152–162. https://doi.org/10.1130/G38513.1.

Dyer B., Maloof A. C. and Higgins J. A. (2015) Glacioeustasy, meteoric diagenesis, and the carbon cycle during the Middle Carboniferous. *Geochem. Geophy. Geosyst.* **16**, 3383–3399. https://doi.org/10.1002/2015GC006002.

Eberli G. P., Swart P. K., Malone M. J., (1997). Shipboard Scientific Party: College Station, TX (Ocean Drilling Program). Proc. ODP Init. Reports 166. doi:https://doi.org/10.2973/odp.proc.ir.166.1997.

Fantle M. S. and DePaolo D. J. (2006) Sr isotopes and pore fluid chemistry in carbonate sediment of the Ontong Java Plateau: calcite recrystallization rates and evidence for a rapid rise in seawater Mg over the last 10 million years. *Geochim. Cosmochim. Acta* **70**, 3883–3904. https://doi.org/10.1016/j.gca.2006.06.009.

Fantle M. S. and DePaolo D. J. (2007) Ca isotopes in carbonate sediment and pore fluid from ODP Site 807A: the Ca^{2+}(aq)–calcite equilibrium fractionation factor and calcite recrystallization rates in Pleistocene sediments. *Geochim. Cosmochim. Acta* **71**, 2524–2546. https://doi.org/10.1016/j.gca.2007.03.006.

Fantle M. S. and Higgins J. (2014) The effects of diagenesis and dolomitization on Ca and Mg isotopes in marine platform carbonates: Implications for the geochemical cycles of Ca and Mg. *Geochim. Cosmochim. Acta* **142**, 458–481. https://doi.org/10.1016/j.gca.2014.07.025.

Farkaš J., Frýda J. and Holmden C. (2016) Calcium isotope constraints on the marine carbon cycle and $CaCO_3$ deposition during the late Silurian (Ludfordian) positive $\delta^{13}C$ excursion. *Earth Planet. Sci. Lett.* **451**, 31–40. https://doi.org/10.1016/j.epsl.2016.06.038.

Geske A., Zorlu J., Richter D. K., Buhl D., Niedermayr A. and Immenhauser A. (2012) Impact of diagenesis and low grade metamorphosis on isotope ($\delta^{26}Mg$, $\delta^{13}C$, $\delta^{18}O$ and $^{87}Sr/^{86}Sr$) and elemental (Ca, Mg, Mn, Fe and Sr) signatures of Triassic sabkha dolomites. *Chem. Geol.* **332**, 45–64. https://doi.org/10.1016/j.chemgeo.2012.09.014.

Ginsburg R. N. (2001) Subsurface geology of a prograding carbonate platform margin, Great Bahama Bank: results of the Bahamas Drilling Project. *SEPM Soc. Sediment. Geol.*, 70. https://doi.org/10.2110/pec.01.70.

Grotzinger J. P. and Reed J. F. (1983) Evidence for primary aragonite precipitation, lower Proterozoic (1.9 Ga) Rocknest dolomite, Wopmay orogen, northwest Canada. *Geology* **11**, 710–713. https://doi.org/10.1130/0091-7613(1983)11<710:EFPAPL>2.0.CO;2.

Gussone N., Böhm F., Eisenhauer A., Dietzel M., Heuser A., Teichert B. M. A., Reitner J., Wörheide G. and Dullo W. C. (2005) Calcium isotope fractionation in calcite and aragonite. *Geochim. Cosmochim. Acta* **69**, 4485–4494. https://doi.org/10.1016/j.gca.2005.06.003.

Hayes J. M. and Waldbauer J. R. (2006) The carbon cycle and associated redox processes through time. *Philos. Trans. R. Soc. B. Biol. Sci.* **361**, 931–950. https://doi.org/10.1098/rstb.2006.1840.

Henderson G. M., Slowey N. C. and Haddad G. A. (1999) Fluid flow through carbonate platforms: constraints from $^{234}U/^{238}U$ and Cl^- in Bahamas pore-waters. *Earth Planet. Sci. Lett.* **169**, 99–111. https://doi.org/10.1016/S0012-821X(99)00065-5.

Higgins J. A., Blättler C. L., Lundstrom E. A., Santiago-Ramos D., Akhtar A., Ahm A-S. C., Bialik O., Holmden C., Bradbury H., Murray S. T. and Swart P. (2018) Mineralogy, early marine diagenesis, and the chemistry of shallow water carbonate sediments. *Geochim. Cosmochim. Acta.* **220**, 512–534. https://doi.org/10.1016/j.gca.2017.09.046.

Higgins J. A. and Schrag D. P. (2010) Constraining magnesium cycling in marine sediments using magnesium isotopes. *Geochim. Cosmochim. Acta* **74**, 5039–5053. https://doi.org/10.1016/j.gca.2010.05.019.

Holmden C., Creaser R. A., Muehlenbachs K., Leslie S. A. and Bergström S. M. (1998) Isotopic evidence for geochemical decoupling between ancient epeiric seas and bordering oceans: Implications for secular curves. *Geology* **26**, 567–570. https://doi.org/10.1130/0091-7613(1998)026<0567:iefgdb>2.3.co;2.

Holmden C., Panchuk K. and Finney S. C. (2012) Tightly coupled records of Ca and C isotope changes during the Hirnantian glaciation event in an epeiric sea setting. *Geochim. Cosmochim. Acta* **98**, 94–106. https://doi.org/10.1016/j.gca.2012.09.017.

Horita J. (2014) Oxygen and carbon isotope fractionation in the system dolomite–water–CO_2 to elevated temperatures. *Geochim. Cosmochim. Acta* **129**, 111–124. https://doi.org/10.1016/j.gca.2013.12.027.

Hu Z., Hu W., Wang X., Lu Y., Wang L., Liao Z. and Li W. (2017) Resetting of Mg isotopes between calcite and dolomite during burial metamorphism: Outlook of Mg isotopes as geother-

mometer and seawater proxy. *Geochim. Cosmochim. Acta* **208**, 24–40. https://doi.org/10.1016/j.gca.2017.03.026.

Hughes J. D., Vacher H. L. and Sanford W. E. (2007) Three-dimensional flow in the Florida platform: Theoretical analysis of Kohout convection at its type locality. *Geology* **35**, 663–666. https://doi.org/10.1130/G23374A.1.

Husson J. M., Higgins J. A., Maloof A. C. and Schoene B. (2015) Ca and Mg isotope constraints on the origin of Earth's deepest C excursion. *Geochim. Cosmochim. Acta* **160**, 243–266. https://doi.org/10.1016/j.gca.2015.03.012.

Irwin H., Curtis C. and Coleman M. (1977) Isotopic evidence for source of diagenetic carbonates formed during burial of organic-rich sediments. *Nature* **269**, 209–213. https://doi.org/10.1038/269209a0.

Jacobson A. D. and Holmden C. (2008) δ^{44}Ca evolution in a carbonate aquifer and its bearing on the equilibrium isotope fractionation factor for calcite. *Earth Planet. Sci. Lett.* **270**, 349–353. https://doi.org/10.1016/j.epsl.2008.03.039.

Jost A. B., Bachan A., van de Schootbrugge B., Brown S. T., DePaolo D. J. and Payne J. L. (2017) Additive effects of acidification and mineralogy on calcium isotopes in Triassic/Jurassic boundary limestones. *Geochem. Geophy. Geosy.* **18**, 113–124. https://doi.org/10.1002/2016GC006724.

Kah L. C. (2000) Depositional δ^{18}O signatures in Proterozoic dolostones: constraints on seawater chemistry and early diagenesis. *Spec. Publ. SEPM* **67**, 345–360.

Kaufman J. (1994) Numerical models of fluid flow in carbonate platforms: Implications for dolomitization. *J. Sediment. Res.* **64A**, 128–139. https://doi.org/10.1306/D4267D2F-2B26-11D7-8648000102C1865D.

Kelts K. and McKenzie J. A. (1984) A comparison of anoxic dolomite from deep-sea sediments: quaternary gulf of california and messinian tripoli formation of sicily. *Pacific Sect. SEPM* **41**, 19–28.

Kim S. T. and O'Neil J. R. (1997) Equilibrium and nonequilibrium oxygen isotope effects in synthetic carbonates. *Geochim. Cosmochim. Acta* **61**, 3461–3475. https://doi.org/10.1016/S0016-7037(97)00169-5.

Kimmig S. R. and Holmden C. (2017) Multi-proxy geochemical evidence for primary aragonite precipitation in a tropical-shelf 'calcite sea' during the Hirnantian glaciation. *Geochim. Cosmochim. Acta* **206**, 254–272. https://doi.org/10.1016/j.gca.2017.03.010.

Kinsman D. J. (1969) Interpretation of Sr concentrations in carbonate minerals and rocks. *J. Sediment. Petrol.* **39**, 486–508, doi:10.1306%2F74D71CB7-2B21-11D7-8648000102C1865D.

Knauth L. P. and Kennedy M. J. (2009) The late Precambrian greening of the earth. *Nature* **460**, 728–732. https://doi.org/10.1038/nature08213.

Knoll A. H., Hayes J. M., Kaufman A. J., Swett K. and Lambert I. B. (1986) Secular variation in carbon isotope ratios from Upper Proterozoic successions of Svalbard and East Greenland. *Nature* **321**, 832–838. https://doi.org/10.1038/321832a0.

Kohout F. A., Henry H. R., Banks J. E. (1977). Hydrogeology related to geothermal conditions of the Floridan Plateau, vol. 21. Florida Department of Natural Resources Bureau of Geology Special Publication.

Kramer P. A., Swart P. K., De Carlo E. H. and Schovsbo N. H. (2000) Overview of interstitial fluid and sediment geochemistry, Site 1003-1007 (Bahamas Transect). *Proc. Ocean Drill. Prog. Sci. Results* **166**, 179–195. https://doi.org/10.2973/odp.proc.sr.166.117.2000.

Kump L. R. and Arthur M. A. (1999) Interpreting carbon-isotope excursions: carbonates and organic matter. *Chem. Geol.* **161**, 181–198. https://doi.org/10.1016/S0009-2541(99)00086-8.

Lau K. V., Maher K., Brown S. T., Jost A. B., Altiner D., DePaolo D. J., Eisenhauer A., Kelley B. M., Lehrmann D. J., Paytan A., Yu M., Silva-Tamayo J. C. and Payne J. L. (2017) The influence of seawater carbonate chemistry, mineralogy, and diagenesis on calcium isotope variations in Lower-Middle Triassic carbonate rocks. *Chem. Geol.* **471**, 13–37. https://doi.org/10.1016/j.chemgeo.2017.09.006.

Lazar B. and Erez J. (1992) Carbon geochemistry of marine-derived brines: I. ^{13}C depletions due to intense photosynthesis. *Geochim. Cosmochim. Acta* **56**, 335–345. https://doi.org/10.1016/0016-7037(92)90137-8.

Malone M. J., Claypool G., Martin J. B. and Dickens G. R. (2002) Variable methane fluxes in shallow marine systems over geologic time: the composition and origin of pore waters and authigenic carbonates on the New Jersey shelf. *Mar. Geol.* **189**, 175–196. https://doi.org/10.1016/S0025-3227(02)00474-7.

Malone M. J., Slowey N. C. and Henderson G. M. (2001) Early diagenesis of shallow-water periplatform carbonate sediments, leeward margin, Great Bahama Bank (Ocean Drilling Program Leg 166). *Geol. Soc. Am. Bull* **113**, 881–894. https://doi.org/10.1130/0016-7606(2001)113<0881:edoswp>2.0.co;2.

Melim L. A., Westphal H., Swart P. K., Eberli G. P. and Munnecke A. (2002) Questioning carbonate diagenetic paradigms: evidence from the Neogene of the Bahamas. *Mar. Geol.* **185**, 27–53. https://doi.org/10.1016/S0025-3227(01)00289-4.

Miller N. R. (1995). Lithostratigraphic signal evaluation of the Miocene Monterey Formation, South Elwood Field, Santa Barbara-Ventura Basin, California. Ph.D. thesis. University of Texas at Dallas. Richardson, TX, United States.

Moore T. S., Murray R. W., Kurtz A. C. and Schrag D. P. (2004) Anaerobic methane oxidation and the formation of dolomite. *Earth Planet. Sci. Lett.* **229**, 141–154. https://doi.org/10.1016/j.epsl.2004.10.015.

Murray S. T. and Swart P. K. (2017) Evaluating formation fluid models and calibrations using clumped isotope paleothermometry on Bahamian dolomites. *Geochim. Cosmochim. Acta* **206**, 73–93. https://doi.org/10.1016/j.gca.2017.02.021.

Panchuk K. M., Holmden C. and Kump L. R. (2005) Sensitivity of the epeiric sea carbon isotope record to local-scale carbon cycle processes: Tales from the Mohawkian Sea. *Palaeogeogr. Palaeoclimatol. Palaeoecol.* **228**, 320–337. https://doi.org/10.1016/j.palaeo.2005.06.019.

Patterson W. P. and Walter L. M. (1994) Depletion of ^{13}C in seawater CO_2 on modern carbonate platforms: Significance for the carbon isotopic record of carbonates. *Geology* **22**, 885–888. https://doi.org/10.1130/0091-7613(1994)022<0885:docisc>2.3.co;2.

Richter F. M. and DePaolo D. J. (1987) Numerical models for diagenesis and the Neogene Sr isotopic evolution of seawater from DSDP Site 590B. *Earth Planet. Sci. Lett.* **83**, 27–38. https://doi.org/10.1016/0012-821X(87)90048-3.

Romanek C. S., Grossman E. L. and Morse J. W. (1992) Carbon isotopic fractionation in synthetic aragonite and calcite: Effects of temperature and precipitation rate. *Geochim. Cosmochim. Acta* **56**, 419–430. https://doi.org/10.1016/0016-7037(92)90142-6.

Rothman D. H., Hayes J. M. and Summons R. E. (2003) Dynamics of the Neoproterozoic carbon cycle. *Proc. Natl. Acad. Sci.* **100**, 8124–8129. https://doi.org/10.1073/pnas.0832439100.

Simms M. (1984) Dolomitization by ground-flow system in carbonate platforms. *Gulf Coast Assoc. Geol. Soc. Trans.* **34**, 411–420.

Stiller M., Rounick J. S. and Shasha S. (1985) Extreme carbon-isotope enrichments in evaporating brines. *Nature* **316**, 434–435. https://doi.org/10.1038/316434a0.

Please cite this article in press as: Ahm A. -S. C., et al. Quantifying early marine diagenesis in shallow-water carbonate sediments. *Geochim. Cosmochim. Acta* (2018), https://doi.org/10.1016/j.gca.2018.02.042

Supko P. R. (1977) Subsurface dolomites, San Salvador, Bahamas. *J. Sediment. Res.* **47**, 1063–1077. https://doi.org/10.1306/212F72DE-2B24-11D7-8648000102C1865D.

Swart P. K. (2008) Global synchronous changes in the carbon isotopic composition of carbonate sediments unrelated to changes in the global carbon cycle. *Proc. Natl. Acad. Sci.* **105**, 13741–13745. https://doi.org/10.1073/pnas.0802841105.

Swart P. K. and Eberli G. (2005) The nature of the $\delta^{13}C$ of periplatform sediments: Implications for stratigraphy and the global carbon cycle. *Sediment. Geol.* **175**, 115–129. https://doi.org/10.1016/j.sedgeo.2004.12.029.

Swart P. and Kennedy M. (2012) Does the global stratigraphic reproducibility of $\delta^{13}C$ in Neoproterozoic carbonates require a marine origin? A Pliocene–Pleistocene comparison. *Geology* **40**, 87–90. https://doi.org/10.1130/g32538.1.

Swart P. K., Ruiz J. and Holmes C. W. (1987) Use of strontium isotopes to constrain the timing and mode of dolomitization of upper Cenozoic sediments in a core from San Salvador, Bahamas. *Geology* **15**, 262–265. https://doi.org/10.1130/0091-7613(1987)15<262:uositc>2.0.co;2.

Swart P. K., Elderfield H. and Ostlund G. (2001) The geochemistry of pore fluids from bore holes in the Great Bahamas Bank. *SEPM Spec. Publ.* **70**, 163–173.

Swart P. K., Eberli G. P., Malone M. J., Sarg J. F. (2000). The oxygen isotopic composition of interstitial waters: evidence for fluid flow and recrystallization in the margin of Great Bahama Bank. Proc. ODP, Sci. Results, 166 doi:https://doi.org/10.2973/odp.proc.sr.166.130.2000.

Swart P. K., Oehlert A. M., Mackenzie G. J., Eberli G. P. and Reijmer J. J. G. (2014) The fertilization of the Bahamas by Saharan dust: a trigger for carbonate precipitation? *Geology* **42**, 671–674. https://doi.org/10.1130/G35744.1.

Tang J., Dietzel M., Böhm F., Köhler S. J. and Eisenhauer A. (2008) Sr^{2+}/Ca^{2+} and $^{44}Ca/^{40}Ca$ fractionation during inorganic calcite formation: II. Ca isotopes. *Geochim. Cosmochim. Acta* **72**, 3733–3745. https://doi.org/10.1016/j.gca.2008.05.033.

Vahrenkamp V. C., Swart P. K. and Ruiz J. (1988) Constraints and interpretation of $^{87}Sr/^{86}Sr$ ratios in Cenozoic dolomites. *Geophys. Res. Lett.* **15**, 385–388. https://doi.org/10.1029/GL015i004p00385.

Vahrenkamp V. C., Swart P. K. and Ruiz J. (1991) Episodic dolomitization of late Cenozoic carbonates in the Bahamas; evidence from strontium isotopes. *J. Sediment. Res.* **61**, 1002–1014. https://doi.org/10.1306/d4267825-2b26-11d7-8648000102c1865d.

Zeebe R. E. and Wolf-Gladrow D. (2001) CO_2 in seawater: equilibrium, kinetics, isotopes. *Elsevier Oceanogr. Ser.* **65**.

Associate Editor: Thomas M. Marchitto